HAWASSA UNIVERSITY INSTITUTE OF TECHNOLOGY
SCHOOL OF ELECTRICAL AND COMPUTER ENGINEERING

ENHANCING THE RELIABILITY OF DISTRIBUTION SYSTEM THROUGH RENEWABLE ENERGY RESOURCES (CASE STUDY: GUDER TOWN DISTRIBUTION SYSTEM)

A THESIS SUBMITED TO THE SCHOOL OF ELECTRICAL AND COMPUTER
ENGINEERING, INSTITUTE OF TECHNOLOGY, SCHOOL OF GRADUATE STUDIES
HAWASSA UNIVERSITY
HAWASSA, ETHIOPIA

IN PARTIAL FULFILLMENT OF THE REQUIREMENT FOR THE DEGREE OF MASTER
OF SCIENCE IN POWER SYSTEM AND ENERGY ENGINEERING

DECEMBER, 2024

HAWASSA UNIVERSITY INSTITUTE OF TECHNOLOGY
SCHOOL OF ELECTRICAL AND COMPUTER ENGINEERING

ENHANCING THE RELIABILITY OF DISTRIBUTION SYSTEM THROUGH RENEWABLE ENERGY RESOURCES (CASE STUDY: GUDER TOWN DISTRIBUTION SYSTEM)

STUDENT
FIRAOL KASAHUN MENGESHA

ADVISOR
DR. YESHITELA SHIFERAW

CO-ADVISOR
MR. ERSTE TELILA (MSC)

HAWASSA UNIVERSITY, ETHIOPIA

DECEMBER, 2024

DECLARATION

I, the undersigned, declare that the thesis comprises my own work. In compliance with internationally accepted practices, I have acknowledged and refereed all materials used in this work. I know that non-adherence to the principles of academic honesty and integrity, misrepresentation/fabrication of any idea/data/fact/source will constitute sufficient ground for disciplinary action by the University and can evoke penal action from the sources, which have not properly cited or acknowledged.

FIRAOL KASAHUN MENGESHA	_____________	_________
Name of student	signature	Date

Place: Hawassa institute of technology, Hawassa University, Hawassa

Date of submission ________________________

This thesis have submitted for examination with my approval as a university advisor

DR. YESHITELA SHIFERAW	_________	___________
Major Advisor	signature	Date
Mr. ERSTE TELILA (MSC)	___________	__________
Co-Advisor	signature	Date

HAWASSA UNIVERSITY

INSTITUTE OF TECHNOLOGY

SCHOOL OF RESEARCH AND POSTGRADUATE STUDIES

FACULTY OF ELECTRICAL AND COMPUTER ENGINEERING

ADVISOR’S APPROVAL SHEET

This is to certify that the thesis entitled “ENHANCING THE RELIABILITY OF DISTRIBUTION SYSTEM THROUGH RENEWABLE ENERGY RESOURCES (CASE STUDY: GUDER TOWN DISTRIBUTION SYSTEM)” Submitted in partial fulfillment of the requirements for the degree of Masters of Science in Electrical Engineering with specialization in “POWER SYSTEM AND ENERGY ENGINEERING”. The Graduate Program of the Department of Electrical and Computer Engineering, and carried out by Firaol Kasahun Mengesha ID No-GPPoSYR/00002/13, under my supervision. Therefore, I recommend that the student has fulfilled the requirements and hence here by can submit the thesis to the department.

DR. YESHITELA SHIFERAW	__________	__________
Major Advisor	signature	Date
Mr. ERSTE TELILA (MSC)	__________	__________
Co-Advisor	signature	Date

HAWASSA UNIVERSITY

SCHOOL OF RESEARCH AND POSTGRADUATE STUDIES

EXAMINER'S APPROVAL SHEET

We the under signed Board of examiners of the final open defence by Firaol Kasahun Mengesha have read and evaluated his thesis entitled "ENHANCING THE RELIABILITY OF DISTRIBUTION SYSTEM THROUGH RENEWABLE ENERGY RESOURCES (CASE STUDY: GUDER TOWN DISTRIBUTION SYSTEM)" and examined the candidate. This is therefore, to certify that the thesis has been accepted in partial fulfilment of the requirements for the masters' degree.

DR. YESHITELA SHIFERAW	___________	____________
Major Advisor	signature	Date
DR. MULUNEH LEMMA	__________	___________
External Examiner	signature	Date
DR. BASEEM KHAN	___________	___________
Internal Examiner	signature	Date
Mr. BEZABIH MOGES	___________	___________
Chair Holder	signature	Date
Mr. DEJENE HURISA	___________	___________
Faculty Dean	Signature	Date
________________________	___________	___________
SGS Approval	signature	Date

Final approval and acceptance of the thesis is contingent upon the submission of the final copy of the thesis to the school of graduate studies (SGS) through the department Graduate Committee (DGC) of Electrical and Computer Engineering.

Stamp of SGS: ___________________

ACKNOWLEDGEMENT

First and foremost, I would like to thanks God, for nothing is possible without his will. Secondly, would like to express my sincere gratitude to my advisor Dr. Yeshitela Shiferaw for his guidance, and encouragement throughout the thesis. I must also express my sincere thanks to the staff of the EEU Guder substation, which provided me with numerous valuable data and for their hospitable service. I would never forget special thanks to my parents; it was never possible without your prayers and support. The tireless prayers of my family and the extraordinary support of my Best Friends Mr. Beharu Bekele and Mr.Getahun shanko enabled me to reach this landmark. Without them, I wouldn't be able to complete my thesis.

TABLE OF CONTENTS

LIST OF TABLES

LIST OF FIGURES

LIST OF ACRONOMYS AND ABBREVATIONS

AENS	Average Energy Not supplied
ASAI	Average Service Availability Index
ASUI	Average Service Unavailability Index
BCBV	Branch Current to Bus Voltage
BIBC	Bus Injection to Branch Current
DG	Distributed Generation
DPEF	Distribution Permanent Earth Fault
DPSC	Distribution Permanent Short Circuit
DTEF	Distribution Temporary Earth Fault
DTSC	Distribution Temporary Short Circuit
EEP	Ethiopian Electric Power
ETAP	Electrical Transient Analysis Program
EENS	Electrical Energy Not Supplied
EEU	Ethiopian Electric Utility
GUI	Graphical User Enter phase
GMR	Geometric Mean Radius
HO	Horizontal Surface
MATLAB	Matrix Laboratory
MTBF	Mean Time between Failures
MTTF	Mean Time to Failure
MTTR	Mean Time to Repair

OPSDG	Optimal Size of Distributed Generation
PSO	Particle Swarm Optimization
RDS	Radial Distribution System
SAIDI	System Average Interruption Duration Index
SAIFI	System Average Interruption Frequency Index

ABSTRACT

The distribution system connects high-voltage transmission networks with end-users. Most of the time, power plants are situated distant from the consumer's location, resulting in large power losses in both the distribution and transmission systems, However, distribution system losses are typically greater than transmission line side losses. The main objective of this study is to reduce power losses and enhance system reliability using Distributed Generation (DG) in the case of the Guder Substation. The Guder Substation has three feeder lines that provide energy for different customers. From these feeders, the Guder town feeder has been chosen since it is frequently interrupted. The chosen feeder has been modeled in ETAP software, and simulation results have been obtained with both ETAP and MATLAB software. The results show that the feeder has a power loss of 611.9843 KW and 323.8237 kVar active and reactive, respectively. Additionally, the study investigates the existing reliability indices of SAIFI, SAIDI, and EENS, which have values of 303.7458 f/cust.yr, 306.4240 hr/cust.yr, and 2368.307 MWhr/yr, respectively. Particle Swarm Optimization algorithm has been suggested to decide the best size and position of DG. After renewable Distributed Generation penetrated the network, the real and reactive power loss reduced from 611.9843 KW and 323.8237 kVar to 302.75 KW and 132.34 kVar, respectively. Additionally, the SAIFI, SAIDI, and EENS system reliability indices were enhanced from 303.7458 f/cust.yr, 306.4240 hr/cust.yr, and 2368.307 MWhr/yr to 27.4968 f/cust.yr, 13.650 hr/cust.yr, and 111.758 MWh/yr, respectively. Finally, reliability indices and line losses before and after Distributed Generations penetrated the network are compared. In general, the simulation results indicate that the suggested method is efficient in maintaining system reliability and minimizing power losses.

Keywords: *Distributed Generation, ETAP, MATLAB, PSO, Reliability enhancement.*

CHAPTER ONE

1. INTRODUCTION

1.1. Background of the Study

The main function of power system is to deliver electrical energy to the customers adequately and efficiently. In other words, the aim of any power system is to provide reliable and affordable electricity to its users. Without proper planning and maintaining reliability, this power has negative economic effects on both the utility and its customers due to cost of interruptions and power outages [1].

Uninterruptible and affordable access to electric power is essential for sustained economic growth and the achievement of high standards of living. Any nation's ability to maintain and develop a modern economy and society depends on a reliable power supply. The most crucial aspect of designing and planning distribution systems that should function efficiently with little disruption of customer loads is reliability assessment.

The system's capacity to provide sufficient electrical energy for the intended amount of time under the actual operating conditions can be used to define reliability. The term "power system reliability" includes all facts of the system's ability to satisfy customers load requirement [2].

1.2. Geographical information of the research area

Guder power distribution is found in Western part of Ethiopia, located in Oromia region west shoa zone. The study area has latitude and longitude of 8.98 norths, and 37.93 easts. Guder power distribution is far away from Addis Ababa at a distance of around 126km, and it supplies electric power to Guder town.

1.3. Statement of the problem

For both utilities and customers, electric distribution systems reliability is important. However, Guder power distribution facing repetitive power outages. Due to a number of factors, the frequent power outages at Guder power distribution have become a serious issue. The human factor, shortage power, equipment failure, extreme weather, and tree are the most factors that lead to distribution system failures. Because of this, all customer i.e. residential, commercial, and industrial sectors are affected with the problem. Power outages are especially difficult to tolerate for industrial sectors, because they result in significant income loss during power outage. Because of this, the reliability of the distribution system has a substantial effect on electricity prices, and satisfaction of the customer. So, in order to enhance utility performance and maintain customer satisfaction, system reliability must be increased. As a result, power distribution companies can reduce costs associated with maintaining and operating distribution systems after a power outage by increasing system reliability.

This study has been focused on distribution system integration with renewable distributed generation to enhance the current system reliability indices of SAIFI, SAIDI, and EENS are 303.7458 f/cust.yr, 306.424 hr/cust.yr, and 2368.307 MWh/yr respectively in order to minimize these system indices values. To overcome these problems, the study considered Photo Voltaic distributed generation which provides a means to beat incremental in energy demand, to enhance distribution system reliability and decrease power loss by generating electric power at the distribution system.

1.4. Objectives

1.4.1. General Objective

The main objective of this thesis is to enhance reliability of power distribution system by integrating distributed generation (DG).

1.4.2. Specific Objectives

The specific objectives of this thesis are: -

- To model and integrate DG to the distribution network by using ETAP software.
- To carry out reliability analysis of the system with optimal placement and size of DGs.
- To examine the impacts of integrating DGs in distribution network, and compare the results before and after DGs integration.

1.5. Significance of the study

The study makes a significant contribution to find the best way to lower distribution losses and enhance reliability. In general, it is believed that this study will be beneficial to both the electric power serving utility, and its customers in;

- ✓ Identifying the primary reasons for power outages and other issues that frequently affect the power distribution system.
- ✓ Enhancing overall system reliability.
- ✓ Preventing the loss of a significant amount of money due to a power outage.
- ✓ Improve the utility and the society's economy.
- ✓ Reduce power supply interruptions.
- ✓ Increase the industrial and commercial sectors.
- ✓ Minimizing distribution losses by allocating DG to the existing network.

1.6. Scope of the study

This research would have focused on studying and analyzing reliability enhancement and power loss reduction in the case of Guder power distribution by integrating distributed generation (DG) to the worst case feeder of the distribution network. Among the Guder substation feeders, Guder town feeder was selected, since it has high interruptions, and frequently outage. Additionally, the study examined the substation's current power system reliability issues, and the percentage of enhancements that can be realized by integrating distributed generation to the existing. System model was developed by ETAP software.

1.7. Limitation of the study

This work has been restricted to reliability enhancement and power loss reduction in the case of Guder power distribution by integrating distributed generation (DG) to the worst case buses of the distribution network. There is no hardware implementation in this work, because it is expensive, time-consuming, and difficult to find the necessary components. System model and simulation studies were conducted by ETAP, and MATLAB software.

1.8. Organization of the thesis

This thesis organized into five chapters as follows:

A brief background, geographic area of the work, problem statement, objectives, significance, research methodology, scope, and research limitation are covered in Chapter one of the research. Chapter two provides information on the theoretical context and a discussion of various previous works which are related to loss reduction and reliability enhancement. Chapter three provides a detailed explanation of the methodology and approaches, starting with a site description, data collection, and analysis. Modeling and simulation of systems were done in Chapter four. Results and discussions have also been conducted in this chapter. Finally, the research's conclusion and recommendations were covered in Chapter five.

CHAPTER TWO

2. LITERATURE REVIEW AND THEORETICAL BACKGROUND

2.1. Introduction

Electrical power is the largest and most complex system, which is a vital element of any modern economy. For economic growth, and development of once country power supply must be available at a fair price. Therefore, the distribution system must be upgraded, and maintained appropriately to meet customer demands. According to a global analysis, around 80% of all customer reliability issues are caused by issues in the distribution system (Mehammed, 2020).

Scheduled and unplanned activities disturb typical working conditions and can cause outages and interruptions. The transmission and distribution system's reliability is assessed using a variety of indicators. The ability to give continuous power for customers at all points of utilization is known as distribution system reliability. In order to achieve power delivery goals and increase customer satisfaction, distribution system reliability is crucial. By reducing the number of interruptions and the length of interruptions, utility profits are generated. For an electrical distribution system, reliability can be interpreted in a variety of ways. These include the availability of the power system and the continuation of services to meet customer demand[4].

2.2. Electrical Power Distribution Systems

Generating stations, transmission lines, and distribution networks work together to produce and deliver electrical energy to customers in cost-effective and reliable manner.

To avoid power outages, the distribution system must be carefully designed, and it can be divided into three main categories. They are radial, ring main, and inter-connected.

2.2.1. Radial Distribution Systems

In a radial distribution system (RDS), lateral-branch circuits and sub feeders help primary feeders transport electricity from the distribution substation to the load areas. Due to its simplicity and low cost of construction, this system is the most widely used [5]. A radial system is vulnerable to numerous interruption possibilities because it is only connected to one source of supply. In comparison to feeders with an alternative supply capability, radial feeders typically have lower reliability. This is the simplest distribution circuit and has the lowest initial cost(Bewketu Getie, 2020).

2.2.2. Ring Main Distribution System

In ring main, the loop circuit starts from the substation bus bars, travels around the area being served, and then returns to the substation. Distribution transformers allow the distributors to be tapped at various locations along the feeder. The main advantage of the ring main system is the consumer terminals less affected by voltage fluctuations.

2.2.3. Inter Connected Distribution System

A system is referred to as interconnected when the feeder node is powered by different generating stations. Through distribution transformers, distributors are connected to the feeder ring points. The benefits of the interconnected system include, any area served by one substation during times of peak load can also be served by the other substation.

2.3. Over View of Distribution System Reliability

Reliability is used to describe a system's capacity to deliver a sufficient amount of electrical energy [7]. In order to achieve power delivery goals and increase customer satisfaction, distribution system reliability is very important. For an electrical distribution system, reliability can be interpreted in a variety of ways.

These consist of the availability and continuity of services that meet customer demand(Mindaye,2020). Every system consists of components that determine and show how well it is working. This unique component consists of two different systems: a parallel system and a series system. The type of system will determine the probability that it will perform well and reliably [9]

Parallel System

With this type of system structure, the issue is that reliability increases less quickly as the number of components rises. Two or more components must simultaneously be in an outage state for the system to be disrupted.

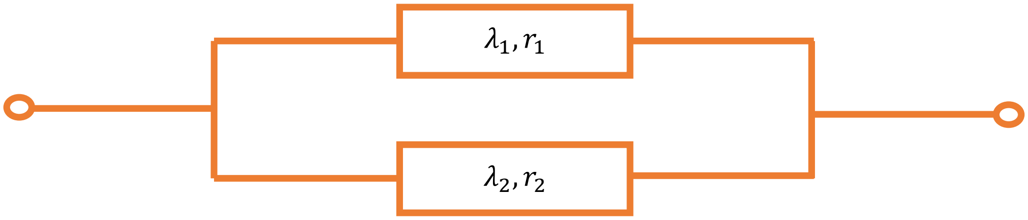

Figure 2.2 Parallel structure[9]

The load point failure modes in this case involve overlapping outages, which means that at least two components must be down simultaneously for a load point to be interrupted, as shown in figure 2.2.

Average failure rate of the system;

$$\lambda p = \frac{\lambda 1\lambda 2(r1 + r2)}{1 + \lambda 1r1 + \lambda 2r2} = \lambda 1\lambda 2(r1 + r2) \tag{2.1}$$

Where λ1r1, and λ2r2 usually <<1

$$\text{Average outage time of the system; } rp = \frac{r_1 * r_2}{r_1 + r_2} \tag{2.2}$$

$$\text{System average annual outage of time; } \mu p = \lambda p * rp \tag{2.3}$$

Where:-

λ_1, and λ_2 are the failure rates and

r_1 And r_1 are the outage times for components 1 and 2 respectively.

Series System

This type of system structure cannot exist unless every component is in a functional state. A radial system is made up of a similar series of parts, including circuit breakers, lines, switches, transformers, and "consumers." In the parallel structure, both parts must fail for the system to stop working, whereas in the series structure, both parts must be intact for the system to function normally.

Figure 2.3 Series structure[9]

Here, as observed in figure 2.3, both are connected in series, and these equations are written as follows:

$$\text{Average failure rate of the system;} \quad \lambda s = \lambda 1 \lambda 2 = \sum_{i=1}^{n} \lambda i \tag{2.4}$$

$$\text{Average Outage time of the system; } rs = \frac{\lambda 1 r 1 + \lambda 2 r 2 + \lambda 1 \lambda 2 + r 1 r 2}{\lambda 1 \, \lambda 2} = \sum \frac{\lambda i r i}{\lambda i} \tag{2.5}$$

$$\text{Average Annual Outage time; } \mu s = \lambda s r s \tag{2.6}$$

Where λi, is the failure rate at node i ri is the outage time at node i.

2.4. Modeling of System Reliability

The reliability indices are commonly used to evaluate the Electric Distribution Network reliability [10], given as follows.

1. Average Failure Rate (λ)

$$\lambda = \frac{\text{Number of outage on component in agiven period}}{\text{Total time component is in operation}} \tag{2.7}$$

2. Mean Time to Failure (MTTF)

The estimated length of time (in years) is that the component will remain in a failed state.

$$\text{MTTF} = \frac{1}{\lambda} = \frac{\text{Total system operating ours}}{\text{Amount of failures}} \tag{2.8}$$

3. Mean Time between Failures (MTBF)

MTBF describes the total time the components in operation. As a result, it expressed as;

$$\text{MTBF} = \frac{\text{Total system operation hours}}{\text{Number of failures}} \tag{2.9}$$

4. Mean Time to Repair (MTTR)

It is the amount of time (in hours) needed to restore an element back to working normally. Usually, it is expressed by r. MTTR = r

It is the typical amount of time required to locate a failure, fix that failure, and return the component to normal operation. It is defined as

$$\mathrm{MTTR} = \frac{\text{Total Duration of outages}}{\text{Frequency of outag}es} = \frac{\text{Total System down time}}{\text{Amount of failures}} \tag{2.10}$$

5. Average Repair Rate (μ):

Mathematically it is the frequency of repair and occurrence per year $\mu = \frac{8760}{\mathrm{MTTR}}$ (2.11)

Availability (U):

The length of time a component is operational at any given time is measured by its availability. It is formulated as;

$$\text{Availability}(\mathrm{U}) = \frac{\mathrm{MTBF}}{\mathrm{MTBF} + \mathrm{MTTR}} \tag{2.12}$$

$$MTBF = MTTF + MTTR/8760 \tag{2.13}$$

2.5. Reliability Analysis Methods

There are two basic approaches used to evaluating distribution system network. These are analytical methods and the Monte Carlo simulation method [11].

2.5.1. Analytical Method of reliability Analysis

A Markov model (analytical method) is one of the techniques used in quantitative reliability analysis and operates with failure frequency (λ), and repair time(r). This approach can be used to assess the reliability of radial systems using a straightforward mathematical formula [12].

2.5.2. Numerical Method

The numerical method is another name for the Monte Carlo simulation technique. This method analyzes the system's random behavior using a simulation of a physical relationship. Contrary to analytical methods, this technique may produce reliability indices with average values as well as expected probability distributions. In a Monte Carlo simulation, system states are randomly selected, tested for acceptability, and then their contributions to reliability indices fall below per-specified tolerances [13].

2.6. Reliability Indices

The given distribution system reliability has been measured using a variety of reliability indices. The reliability indices represent the sum of the reliability data, which may have been gathered from customers, feeders, or loads. These indices are determined by taking into account the entire distribution system's average duration, frequency, customers number, connected load, and power interruptions. Based on system topology and component failure data, this predicts the future performance of the system (Bewketu Getie, 2020).

Power is delivered via a distribution system from a substation to specific customer load points. The degree of service continuity can be described using three fundamental reliability indices. The average annual unavailability time (U), as well as the load point average failure rate (λ), and average outage time (r). The average failure duration at the load point is the average outage time. The average annual outage time is the sum of all outages experienced at the load point over the year. These reliability indices are expected values and reflect average values over the long term(Bewketu Getie, 2020).

2.6.1. System Reliability Indices

An overall distribution system with system reliability indices can be used to evaluate the overall system performance. In addition to the fundamental reliability indices, system-oriented and energy-oriented reliability indices are needed to fully understanding the system. These system-oriented indices: System Average Interruption Frequency Index (SAIFI), System Average Interruption Duration Index (SAIDI), Customer Average Interruption Duration Index (CAIDI), Average System Availability Index (ASAI), Average System Unavailability Index (ASUI), and energy oriented indices namely: Energy Not Supplied(ENS), Average System Interruption Frequency Index (ASIFI), Average System Interruption Duration Index (ASIDI) [14].

1. **System Average Interruption Frequency Index (SAIFI)**

This index measures the typical number of sustained customer interruptions encounters in a unit of time (generally 1 year). SAIFI measurement can be calculated as: -

$$\text{SAIFI} = \frac{\text{Number of customers interrupted}}{\text{Number of customers served}} \; (\frac{\text{f}}{\text{cust}}/\text{yr}) \tag{2.14}$$

2. System Average Interruption Duration Index (SAIDI)

This index shows the typical number of customer interruptions experiences over the time cycle (1 year). The indices are typically expressed interruption hours per year for customers. It is calculated by dividing the total number of customer interruptions over a year by the total number of customer served. SAIDI measurement is calculated as –

$$\text{SAIDI} = \frac{\text{sum of interruption durations of customers}}{\text{Total number of customer served}} \; (\frac{\text{hr}}{\text{yr}}) \tag{2.15}$$

3. Customer Average Interruption Duration Index (CAIDI)

The CAIDI shows the typical amount of time needed to restore the service. It is calculated by dividing the total number of customer sustained interruptions over a one-year period by the total number of customer sustained interruptions.

$$\text{CAIDI} = \frac{\text{sum of customer interrruption durations}}{\text{Total number of customer interruptions}} = \frac{\text{SAIDI}}{\text{SAIFI}} \, (\text{hr}) \tag{2.16}$$

4. The Average Service Availability Index (ASAI)

ASAI specifies the percentage of time that a customer has power during the predetermined period of time. ASAI is calculated as,

$$\text{ASAI} = \frac{\text{customer hours of available service}}{\text{customer hours demanded}} \tag{2.17}$$

5. Average Service Unavailability Index (ASUI)

ASUI is the percentage of time customers run without electricity over a predetermined period of time. It is stated as,

$$\text{ASUI} = (100\text{-ASAI})\text{or}\text{ASUI} = \frac{\text{Duration of outage in hourse}}{\text{Total hours demanded}} = \frac{8760-\text{SAIDI}}{8760} = 1 - \text{ASAI} \tag{2.18}$$

2.6.2. Energy Oriented Reliability Indices

The average load at each load point is one of the most crucial parameters needed for the evaluation of load and energy-oriented indices. The load and energy indices are expressed in the following formula:

1. Energy Not Supplied Index (ENS)

ENS details the typical energy that the customer has not received in the designated time. The failure rate, typical outage duration, and annual unavailability are the three fundamental system indices connected to system load points. This index displays the overall energy that the system is not supplying. And it's provided by,

$$\mathrm{ENS} = \sum \mathrm{La(i)\ Ui} \tag{2.19}$$

Where, La (i) is the average load given by:

$$\mathrm{La(i)} = \mathrm{LP(i)} \times \mathrm{LF(i)} = \frac{\mathrm{Ed}}{\mathrm{t}} \tag{2.20}$$

Where, Lp =peak load, Lf =load factor, Ed= average energy and T=time required.

2. Average Energy Not Supplied Index (AENS)

This index represents the typical energy that the system does not supply.

$$\mathrm{AENS} = \frac{\text{Total energy not supplied}}{\text{Total number of customer served}} = \frac{\sum \mathrm{La(i)Ui}}{\sum \mathrm{Ni}} \tag{2.21}$$

2.7. Reliability enhancement Techniques

In order to achieve better reliability results, it is crucial to implement the mitigation techniques after developing the reliability enhancement strategy. Therefore, it is crucial to identify the root cause and apply mitigation strategies. The distribution system is directly impacted by the electrical mitigation strategies, which also have an impact on the distribution system analysis. These techniques can be done by,

- Install various distributed generation
- Applying distribution system protection
- Decreasing system automation and equipment failure
- FACTS devices usage and etc.

2.7.1. Distributed Generation (DG)

DG is a small-scale power generation technology that connects to consumer loads via a utility's distribution network in order to deliver electricity at a location that is more convenient for customers than a central station generation. A novel method based on renewable energy sources called distributed generation (DG) has the potential to be a vital component of the future electric power system [15].

2.7.2. Distributed Generation Technologies

The two types of distributed generation technologies are non-renewable and renewable, which as depicted in figure 2.4. There are various distribution generation technologies in each form (Adefarati And Bansal 2017; Bewketu Getie 2020).

A. Non-Renewable DG Technologies

Non-renewable technologies generate energy for various operations using fossil fuels such as natural gas, coal, and petroleum. Non-renewable resources cannot be replaced by natural means and are not sustainable. Due to the high rate of energy demand from non-renewable energy resources and the rate of regenerating them within the Earth, they will eventually run out of use. Reciprocating engines, gas turbines, micro-turbines, and steam turbines are some non-renewable energy sources[17].

B. Renewable DG Technology

Fuel Cells

Fuel Cells (FC) classified under the category of unconventional generators. They are electro chemical devices that combine oxygen and hydrogen without combustion to convert chemical energy from a fuel directly into electrical energy [18]. This electrochemical reaction produces high-current, low-voltage DC power.

Photovoltaic

Photovoltaic (PV) generation is a renewable energy source technology, which converts sunlight directly into electricity. PV based DG systems can be easily integrated into a variety of locations, including, distribution networks, buildings and rooftops. The forward potential drop across the semiconductor p-n junction regulates the generated voltage potential. The surface area and density of the solar power radiation both affect how much current is generated [18].

Wind Turbines

One of the most well-liked renewable energy sources in the world is wind power. A wind farm is typically created by combining several wind turbines that have been integrated to the distribution voltage level. Wind turbines, like PV systems, don't use fuel, emit no emissions, and generate DC power. High initial costs and unpredictable energy production are the main drawbacks of wind turbines. Additionally, they are inappropriate for CHP applications [18].

2.7.3. Benefits of Renewable Distributed Generation on Distribution System

DG is a small-scale power generation technology that is connected to consumer loads and used to generate electricity at a location closer to the consumer than a central station. A novel method based on renewable energy sources called distributed generation (DG) has great potential in future electrical power. As a result, incentives, flexibility, gas emission free operation, and energy resource recycling make distributed generation the most preferable energy source. Additionally, DG has benefits in terms of economic, technical, and environmental considerations[17].

A. Impact of Renewable DG in Distribution System Reliability

In order to meet the rising demand for electricity and boost the reliability of the power system, researchers are concentrating on creating distributed generation systems that are practical, affordable, and time-saving. The power system is significantly impacted by distributed generation, which changes the flow of power and reliability factors. The effects of distributed generation on the distribution system's reliability would include increased reliability, financial gains, and reduced environmental pollution. Most of the time distributed generation is placed close to customer premises to enhancing maximum reliability, allowing for the most access to customer numbers (Bewketu Getie, 2020).

B. Benefits of DG on Power Loss Reduction

Reducing the system's electrical power losses is one of the main justifications for integrating renewable DG units. If renewable DG units are integrated into the distribution system, the amount of current flowing in the feeders or other areas of the network will be reduced to a specific percentage. The effect of renewable distributed generation (DG) on power losses depends on the DGs size, location, load size, and network configuration(Bewketu Getie, 2020).

C. Economic Benefits of Renewable DG

Since renewable DG is located at or close to load points, the economic benefits of renewable DG penetration can be attained by omitting any investment cost on the distribution and transmission system. Integration of renewable DGs reduces power system losses that should have been transmitted to consumers as high energy costs. The cost of generating electricity must be lower than the cost of selling it for a power plant to be optimally and economically viable (Bewketu Getie, 2020). The benefit-to-cost ratio can be used to estimate the economic benefits of using renewable DG in the distribution system [19].

2.8. Previous Related Works

This work, [20] analyzed sensitivity based method for optimal placement of distributed generation in order to improving the voltage profile and power loss in the power system network. The study was used Loss sensitivity and Voltage sensitivity index, and it has been concluded that loss reduction in loss sensitivity method is more and it is better in terms of selecting the optimal location for the placement of DG. However, the study does not consider the reliability issue, and investment cost required to install the DG. Again this work does not considered types of DG, and its power factor.

In this study [21], the researchers attempted to increase system efficiency by integrating various DG capacities into a radial distribution feeders. In this case, the outcomes have been mathematically analyzed, and the simulation was taken by ETAP software. The drawback of this work is, it does not considered cost analysis rather than integrating many DG to the network.

This study [22] presents an appropriate method for DG sizing and placement that will reduce line losses, increase voltage profile, and improve system stability. In this work, based on sensitivity methods, the sensitive buses were chosen for optimal DG allocation and size by using quadratic curve-fitting method. In this case, different DG units have been considered. System modeling and simulation results have been performed by MATLAB/PSAT tool box software. However, this research does not study power system reliability.

The main objective of this study[23] was, to find optimal size and placement of solar PV to improve voltage profile at all the nodes, and reduce power losses in radial distribution network using particle swarm optimization algorithm. In this study, two scenarios were taken into account. The integration of a single DG was scenario one, and the integration of two DGs was scenario two. Furthermore, results obtained indicate that adding more DGs improves voltage at each node of the radial distribution network, and lowers losses. But this study does not considered reliability of the system; it only focused on power loss and voltage profile issues.

This paper [10] has performed research on "Reliability Evaluation of Distribution Network with Different Distributed Generators." In this study, by analyzing the reliability models of various DGs, reliability analysis for distribution networks with multiple - types of DG was proposed, and the multi-state model for DG output power was carried out. The simulation results indicate that the suggested approach is practical, simple, and reliable. In this study, different scenarios were considered with installing three DG’s having different sizes. But, Investment cost required to install the DG was not calculated, and also DG type was not taken into account, and also the effect of DG on power losses does not taken into account.

This paper [24] used an analytical method based on an outage data obtained from the northern region of electric power utility office, Maychew distribution system reliability was assessed. Five feeders' monthly reliability for 2011E/C was assessed. Generally, the researcher come to the conclusion as the distribution performs poorly. The drawback of this study was, it does not considered the enhancement issues rather than analyzing the existing system. In addition to this, only one-year data was analyzed.

This research [25] determine the best locations and size of distributed generation in distribution network with ant colony optimization method. The result obtained shows that voltage profile, and total power loss of the distribution network was improved significantly with ACO-based approach. Therefore, the researcher suggested that rather than using non- renewable DG source, various types of renewable energy DG sources must be expanded. Therefore, in this case, the integrated DG is not renewable DG source; it was generic DG source.

This study [26] analysis the impact of Distributed Generation on the reliability of distribution system. In this work, five injection substations were used as case studies. With and without DG units, the network's reliability was examined. When DG units were integrated into the network at various locations, the network's reliability increased. The system's reliability was further increased by multiple DG integration into the network close to load points. The drawback of this study is, it does not consider the impact of DGs on power losses, and DG cost was not analyzed.

The study [21] obtained reduced line losses for a radial distribution system by allocating a distributed generator at a specific location. The results show that as DG integration increases, line losses decrease in accordance with load rating. The DG integration is also influenced by the terminal voltage, phase, and synchronization frequency. This study focused only on power loss reduction.

In this study,[27] the performance of a 33/11KV substation using distributed generation (DG) units was examined in order to address issues with power losses and low voltage profiles. In addition to this, injection substation transformers are also upgraded for adequate power flow without overloading the transformers. The analysis ensures that adequate placement of DG and optimal size is investigated and adopted. In general, this research's findings indicated a significant reduction in power losses and voltage stability. But, the study does not consider reliability issues.

This study [28] focused on reducing power losses and improving the reliability of the Radial Distribution System after it was reconfigured with the placement of Distribution Generation. In this case, the LSF method was used to determine the best switch combinations and DG placements in order to minimize losses. The drawback of this work is, cost to implement is high, because it requires additional switches in addition to multiple DGs. In addition to this, optimal DG sizing and placement was carried out by analytical method.

In this work,[29] a placement selection method for DGs was used, with the goal of minimizing power loss. Then, with the placement of 1-DG and 2-DG, the results were obtained. It was concluded that, the placement of the DG was found to have improved the voltage profile and decreased system losses. However, the study does not consider reliability of the system, and also cost analysis of the installed DG was not estimated, DG-type not discussed.

This paper [30]contributes an analytical method allocation and size selection of distributed generations for radically distribution systems. Comparing the proposed technique to other methods, it is computationally faster. Improve voltage profiles at each node and a decrease an overall active power loss was the main objective of this work. In this work, Voltage stability indicator (VSI) was used to identify the loaded bus in the system. The bus with the highest load was chosen as the best location for the DG. The continuous increment of step size (CISS) technique was used to determine the size of the DG at identified location. However, the study does not considered reliability enhancement, and also DG placement and sizing was done by analytical method.

This work[20] provides a sensitivity-based method to allocating distributed generation with the goal of improving voltage profile and reducing power losses to narrow the gap between power produced and required by consumers. In this study, 153 kW DG was assigned to bus 5 using the Loss Sensitivity Method, brings power reduction by 46% and an improve voltage profile. At each node, the voltage sensitivity index was calculated, and bus 17 was found to have the minimum VSI. In this case, DG sizes were tested at various power factors of 1.0, 0.9, 0.85, and 0.8 in steps of 17.5 kW, ranging from 30 kW to 170 kW. In this study, reliability of the system was not studied, and DG installation cost and type was not taken into account. Additionally, optimal DG placement and sizing must be carefully done with the consideration of different types of DG.

Generally, the above listed literatures explain that reliability enhancement of distribution networks with DGs has drawn attention of researchers in power systems engineering. Many researchers have analyzed distribution systems with renewable resources such as solar and wind energy in order to implement these resources in reliability studies. Reliability assessment of distribution system is required for secure and adequacy of power system distribution and minimum operating cost of utility. To evaluate it, the way of reliability evaluation of distribution system and reliability indices plays the major tasks. However, research or review articles reported so far on power reliability enhancement did not give a great emphasis to the effect of DGs on power losses in the network. This thesis therefore, gave due attention to the mentioned gap above by considering the impact of DGs on power losses.

Some of the related works have considered optimization of power system distribution network through power loss and voltage stability enhancement using different optimization algorithm. However, distribution network optimization (power loss minimization) with considering DGs investment cost is their own gap. In addition, some research has not considered algorithm for DGs placing and sizing rather than using analytical method while penetrating to the distribution network. In order to alleviate the gaps observed in the aforementioned reviews, this thesis work proposed backward forward sweep load flow analysis with particle swarm optimization method to find the optimal size and placement of DGs in radial distribution system for the selected feeder using MATLAB software.

All the above literatures have their own gaps as indicated or discussed under each paper reviewed. This research is therefore targeted to fill these gaps by using Particle Swarm Optimization algorithm. Moreover, no assessment or no any research work has been carried out to address the existing issues on the Guder power distribution so far.

CHAPTER THREE

3. DATA COLLECTION AND ANALYSIS

3.1. Introduction

A complete set of reliability indices, such as SAIFI, SAIDI, CAIDI, ASAI, ASUI, ENS, AENS, etc., describe the reliability of a distribution system. Two years recorded data of interruptions, and other factors are considered for evaluating reliability. The distribution system data that have been gathered and are required for reliability assessment are presented in this chapter.

These data are analyzed to identify the current reliability status of the selected feeder and to identify the main problems of interruption. Generally, the following methodology has been followed in conducting data collection:

Literature review: - Numerous published sources on reliability analysis and power loss minimization have been examined in a variety of books, articles, unpublished papers, and other materials.

Data collection: - In order to complete this thesis, various data have been gathered from National Meteorological Agency, EEU, EEP, and customer utility services.

In this thesis work, the data has been collected through various methods like surveys, observations, personal interviews and technical collection from the site and concerned offices. The collected data include: Interruption data, distribution transformers with their rating, line length between buses, real, and reactive power at each node, conductor type, resistance and reactance of conductor, and sunshine data of the selected area. In case of data collection, QGIS, and RET Screen software is used for conductor impedance determination, and resource available at the selected site respectively.

3.2. Data Collected from Guder Substation

Data from EEU has been gathered for the analysis. Data that was gathered and recorded include fault types, interruptions frequency and duration of outgoing feeders, line data, load data, population size and etc. The gathered data from the substation is data of two years (2021 and 2022). In the context of this study, Guder has three outgoing feeders namely, Ambo town feeder, Guder town feeder, and Ambo mineral water feeder.

All necessary information data was collected from district utility office, substation station, customer service centers, and summarized as follows;

Table 3.1 Guder Substation Overview

Name of Substation	Voltage (kV)	Transformer Number	Transformer Power (MVA)	Incoming Feeder
Guder	132KV/15KV	1	50	Gedo

In Table 3.2 below, the all low voltage transformers' system loads currently available at work site, and other important data’s are listed.

Table 3.2 General over view of the feeders

Feeder Name	Guder town	Ambo town	Ambo mineral water
Voltage Level (KV)	15	15	15
Peak Load (MW)	7.5	8.48	3.04

Table 3.3 Total capacities and customer’s data connected to each transformer of the feeder

S/N	Transformer ID	Rating in (KVA)	Total Customer connected	Peak load (KW)	Peak load (KVAR)
1	DT-012505	200	107	60	45
2	DT-012500	630	437	337.8	253.35
3	DT-012518	315	156	111	83.25
4	DT-012509	25	17	14	10.5
5	DT-012511	200	97	49	36.75
6	DT-012512	200	94	61	45.75
7	DT-012508	200	84	53	39.75

8	DT-012515	100	69	41	30.75
9	DT-012516	100	74	45	33.75
10	DT-012517	50	53	13	9.75
11	DT-012514	25	15	12	9
12	DT-012519	50	30	9	6.25
13	DT-012520	100	60	45	33.75
14	DT-012521	100	65	33	24.75
15	DT-012522	100	68	25	18.75
16	DT-012473	315	172	123.6	92.7
17	DT-012479	630	470	363	272.25
18	DT-010481	315	164	117.3	87.9
19	DT-012480	200	104	69	51.75
20	DT-012481	100	73	31	23.25
21	DT-012483	315	180	129.9	97.4
22	DT-012484	200	114	77	57.75
23	DT-012485	50	37	15	11.25
24	DT-012486	100	45	21	15.75
25	DT-012491	315	226	153.3	114.9
26	DT-012492	315	375	287	215.25
27	DT-012493	50	32	11	8.25
28	DT-012494	315	374	286.6	214.95
29	DT-012495	315	405	311.4	233.55
30	DT-012496	630	641	487.4	365.55
31	DT-012497	100	40	17	12.75
32	DT-012498	25	16	13	9.75
33	DT-012499	100	62	35	26.25
34	DT-012506	315	250	186.2	139.65
35	DT-012501	315	361	261.8	196.35
36	DT-012502	315	297	244.4	168.3

37	DT-012503	800	397	305	228.75
38	DT-012504	315	195	142.5	106.8
39	DT-012676	100	42	17	12.75
40	DT-012808	50	38	16	12
41	DT-012809	630	406	212.6	134.45
42	DT-012810	315	211	155	116.3
43	DT-012811	800	317	241	180.75
44	DT-012812	200	124	85	63.75
45	DT-012813	100	70	27	20.25
46	DT-012814	315	148	104.7	78.5
47	DT-012815	50	25	20	15
48	DT-012816	25	12	10	7.5
49	DT-012818	200	134	93	69.75
50	DT-012819	315	159	98.4	93.8
51	DT-012820	315	133	92	69
52	DT-012822	100	37	15	11.25
53	DT-012824	200	74	45	33.75
54	DT-012825	100	47	23	17.25
55	DT-012859	315	135	79.5	59.6
56	DT-012866	200	69	41	30.75
57	DT-012867	315	102	66.9	50
58	DT-012827	200	60	33	24.75
59	DT-012828	200	144	101	75.75
60	DT-012831	25	14	11	8.25
61	DT-012832	315	245	167.7	127.7
62	DT-012833	315	188	123.2	92.15
63	DT-012834	50	22	18	13.5
64	DT-012835	200	69	41	30.75
65	DT-012840	100	85	39	29.25

66	DT-012843	630	344	162.2	96.6
67	DT-012845	200	213	157	117.75
68	DT-012868	200	243	181	135.75
69	DT-012870	200	228	169	126.75
70	DT-012873	315	174	111	83.25
71	DT-012875	25	11	9	6.75
72	DT-012876	100	72	43	32.25
73	DT-012869	200	55	29	21.75
74	DT-012890	200	50	25	18.75
75	DT-012891	100	48	9	6.75
76	DT-123444	315	109	73.2	54.9

3.2.1. Impedance Calculation of Overhead Medium Line

Type and length of conductor used is the primary data needed for this study. The stranded conductor types used in the Guder town feeder are $\text{AAC} - 50mm^2$, and $\text{AAC} - 95mm^2$. Hence, dividing the impedance per kilometer by the length of the line, positive sequence impedances for the line sections are calculated.

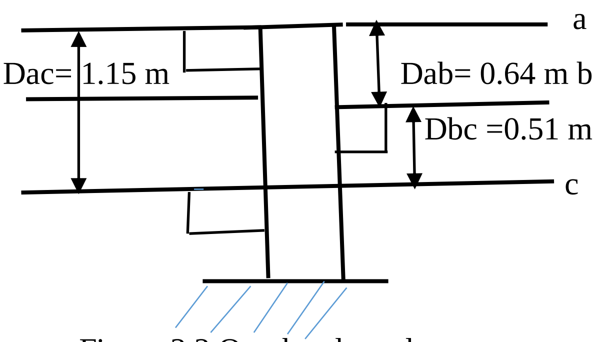

Figure 3.2 Overhead conductor arrangement (by researcher)

Table 3.4 Overhead medium voltage conductor size

Conductor type	Nominal area (mm^2)	Actual area (mm^2)	Wire diameter and Strand	Over all diameter (mm)	Actual diameter (mm)	Resistanc (Ω/km)	GMR (mm)
AAC-50	50	49.48	7/3	9	7.9377	0.5785	2.88
AAC-95	95	93.27	19/2.5	12.5	10.8975	0.3085	4.129

The parameters of the overhead conductors are listed in Table 3.5 below; the conductor resistances were taken from the standard overhead conductor data sheet, and Equation 3.1 given below is used to calculate the GMRs.

GMR for stranded conductors is defined as:

$$GMR = k.\ r \tag{3.1}$$

Where: k = GMR factor, and r = actual conductor radius.

Table 3.5 GMR factor (k) and strand relationship for AAC conductor

Strands	1(solid)	3	7	19	37	61
GMR factor(k)	0.7788	0.6778	0.7256	0.7577	0.7678	0.7722

By having the above given data, mutual and self-impedances are given by:

$$Zii = ri + j0.062832ln\frac{1}{\text{GMRi}}\ \Omega/km \tag{3.2}$$

$$Zij = j0.062832ln\frac{1}{\text{Dji}}\ \Omega/km \tag{3.3}$$

Where:-

Zii = conductor's self-impedance in ohm per kilometers.

Zij = mutual impedance between conductors i and j in ohm per kilometers

ri = conductor resistance in per kilometers, and

Dij= is the measured distance between conductors i and j.

From Table 3.5 and applying Equations 3.2 and 3.3, results the following.

1. The self-impedance for phase conductors of AAC-95mm^2 conductor type

$$Zaa = ra + 0.049348 + j0.062832\ln(\frac{1}{\text{GMRa}} + 6.837026)\ \Omega/km \tag{3.4}$$

$Zaa = 0.3085 + 0.049348 + j0.062832\ln(\frac{1}{0.004129} + 6.837026\ )\Omega/km$

$Zaa = 0.357848 + j0.774514\ \Omega/km$

$Zaa = Zbb = Zcc$

Applying Equation (*3.3*), mutual impedances can be calculated as follows,

$$\text{Zab} = 0.049348 + \text{j}0.062832\ln(\frac{1}{\text{Dab}} + 6.837026)\ \Omega/\text{km} \tag{3.5}$$

$Zab = 0.049348 + j0.062832\ln(\frac{1}{0.64} + 6.837026)\ \Omega/km$

$Zab = 0.049348 + j0.457625\ \Omega/km$

$$Zac = 0.049348 + j0.062832\ln(\frac{1}{\text{Dac}} + 6.837026)\ \Omega/km \tag{3.6}$$

$ac = 0.049348 + j0.062832\ln(\frac{1}{1.15} + 6.837026)\ \Omega/km$

$Zac = 0.049348 + j0.420802\ \Omega/km$

$$ZbA = \pi r^2 c = 0.049348 + j0.062832\ln(\frac{1}{\text{Dbc}} + 6.837026)\ \Omega/km \tag{3.7}$$

$Zbc = 0.049348 + j0.062832\ln(\frac{1}{0.51} + 6.837026)\ \Omega/km$

$Zbc = 0.049348 + j0.471892\ \Omega/km$

Using Equations (3.4)-(2.21), the positive sequence impedance can be calculated. The self - impedance is:

$$Zs = \frac{1}{3}(Zaa + Zbb + Zcc)\Omega/km = (0.357748+\text{j }0.774514)\ \Omega/km \tag{3.8}$$

Mutual impedance is:

$$Zm = \frac{1}{3}(Zab + Zbc + Zac)\Omega/km \tag{3.9}$$

$= \frac{1}{3}((0.049348 + j0.457625) + (\ 0.049348 + j0.471892) + (0.049348 + j0.420802))\Omega/km$

$= 0.049348 + \text{j}0.450106\ \Omega/km$

Positive sequence impedance (+Z) of AAC $-$ 95 is obtained as:

$$Z+= \text{ Zs} - \text{Zm}\ \Omega/km \tag{3.10}$$

$Z+= \ (0.357748 + \text{j }0.774514) - (0.049348\ +\ \text{j}0.450106\ )\ \Omega/km$

$= \ 0.3085+\text{j}0.3244\ \Omega/km$

2. For AAC-50mm^2 conductor type

To obtain the impedance of the feeder for AAC-50 conductor type, the same process and equations are used as in AAC-95.

$$Z+= \text{Zs} - \text{Zm}\ \Omega/km \tag{3.11}$$

$Z+= \text{Zs} - \text{Zm}\ \Omega/km$

$= (0.627848+j0.797149) – (0.049348+j0.450140)\ \Omega/km$

$= 0.5785+j0.3470\ \Omega/km$

Finally, the line impedance (resistance, and reactance) were calculated and tabulated in Table given in Appendix D.

3.2.2. Factors that Causes Power Outages in the Guder Substation

Earth faults and short circuits are the most common major faults in Guder substation. Additionally, scheduled interruptions occur for maintenance and operational reasons. The main faults that are present can be either momentary or sustained in nature. There are two types of interruptions: planned and unplanned interruptions. Construction, preventative maintenance, and repairs are the main reasons for planned interruptions. When an interruption is planned, it happens at a less disruptive time for the customers and they are informed in advance. Unplanned interruptions can occur for a variety of reasons, such as the clearing of faults, unintended the protective system operating, or an unintended human action causing a switching device to open.

Distribution Earth fault

A conducting connection between an electric conductor and a material that; is grounded or has the potential to become grounded results distribution earth fault. In a ground fault, electricity travels to the ground along a path that was not intended for it, like through a person's body.

The earth fault is a plant engineering issue that results from insulating loss between an exposed conductive portion and a live conductor. It may result total damage.

Distribution Short Circuit

The most frequent description of a power outage's root cause is short circuit. It happens when an electrical current flows through a circuit in a different direction than it was intended to. This results in an excessive electric current that can damage circuits and cause fires and explosions. In actuality, short circuits are among the main reasons for electrical fires all over the world. Additionally, it happens when the wiring's insulation fails.

3.2.3. Power Interruption Data

Interruptions frequently happen as the system responds to a fault. Guder distribution system is faced by earth faults and short circuits. These faults can be divided into two categories: temporary faults and permanent faults. The majority of faults in distribution systems are temporary[31]. As shown in Tables 3.6 below, the collected interruption data are condensed for two years of annual power outages with full frequency and duration interruption.

Table 3.6: Frequency and duration of interruptions at the selected site

Year	Name of feeder	Reason of interruptions										Total interruption (Forced+op)	
		DPEF		DPSC		DTEF		DTSC		OP			
		F	D(H)	F	D(H)	F	D(H)	F	D(H)	F	D(H)	F	D(H)
2021	Ambo water	2	17.55	36	68.13	6	1.89	24	13.58	43	68.06	111	169.31
	Guder town	17	27.32	78	108.76	17	21.05	98	33.36	113	89.43	323	279.92
	Ambo	20	41.32	95	130.48	15	13.29	79	13.69	78	74.58	287	263.36
2022	Ambo water	17	32.41	28	51.11	4	0.25	17	4.65	86	136.31	152	224.73
	Guder town	33	71.03	119	143.84	35	31.85	76	39.17	124	108.08	387	393.97
	Ambo	64	95.16	162	221.12	17	1.53	34	2.63	78	56.84	355	377.28
Av. 2021 and 2022	Ambo water	9.5	24.98	32	59.62	5	1.07	20.5	9.115	64.5	102.185	131.5	197.02
	Guder town	25	49.175	98.5	126.3	26	26.45	87	36.265	118.5	98.755	355	336.945
	Ambo	42	68.24	128.25	175.8	16	7.41	56.5	8.16	78	65.71	321	320.32

According to Table 3.6 above, the frequency and duration of interruptions for Ambo mineral water and Ambo town feeders are less frequent and shorter than Guder town feeder. In other words, Guder town feeder is more frequent and longer duration interruptions than others.

Due to the time and its complexity, the study is restricted on one feeder. Out of the mentioned feeders above, Guder town feeder has been chosen for my study of reliability evaluation in this thesis. Because this feeder service many government, and non-government universities, Hospitals, factories, and different commercial centers in addition to domestic customers. And also this feeder has high frequency and duration of interruptions as compared with other feeders of the substation.

Table 3.7: Guder town feeder interruption data in 2021

Year.	Name of feeder	Main reason of interruptions										Total interruption (Forced+op)	
2021		DPEF		DPSC		DTEF		DTSC		OP			
		F	D(H)	F	D(H)	F	D(H)	F	D(H)	F	D(H)	F	D(H)
	Guder town	17	27.32	78	108.76	17	21.05	98	33.36	113	89.43	323	279.92

According to Table 3.7, the main causes of interruptions in the distribution system are short circuit faults and operational needs. Earth faults and short circuit faults are the major types of faults that frequently happen in this distribution system.

Table 3.8 Guder town feeder interruption data in 2022

Year.	Name of feeder	Main reason of interruptions										Total interruption (Forced+op)	
2022		DPEF		DPSC		DTEF		DTSC		OP			
		F	D(H)	F	D(H)	F	D(H)	F	D(H)	F	D(H)	F	D(H)
	Guder town	33	71.03	119	143.84	35	31.85	76	39.17	124	108.08	387	393.97

According to Table 3.8, the duration and frequency of interruptions in the Guder town feeder were high in 2022. The duration and frequency of interruptions were relatively lower in 2021.

From Table 3.7 and Table 3.8 the average interruption duration and frequency of the two years' period by taking the contribution of each type of faults can be calculated.

Table 3.9 Average interruption frequency and duration of Guder feeder in year 2021 and 2022

Year.	Name of feeder	Main reason of interruptions										Total interruption (Forced+op)	
Av. 2021& 2022		DPEF		DPSC		DTEF		DTSC		OP			
		F	D(H)	F	D(H)	F	D(H)	F	D(H)	F	D(H)	F	D(H)
	Guder town	25	49.175	98.5	126.3	26	26.45	87	36.265	118.5	98.755	355	336.945

Based on Table 3.9, it is possible to determine percentage contribution that each type of interruptions on duration and frequency over the two years' period, and tabulated as Table 3.10, and Table 3.11 below.

Table 3.10 Percentage contribution of each type of outages in frequency and duration

	DPEF		DPSC		DTEF		DTSC		OP	
Percentage frequency & duration	F	D(H)	F	D(H)	F	D(H)	F	D(H)	F	D(H)
	7.0423	14.6	27.75	37.484	7.32	7.85	24.51	10.763	33.38	29.31

Table 3.10 Shows that the types of outages due to short circuits (both permanent and temporary), and operation is taking larger percentage when compared to earth faults.

Table 3.11 Percentage of outages in terms of frequency in two years

	DPEF	DPSC	DTEF	DTSC	OP
% frequency	7.0423	27.75	7.32	24.51	33.38

As observed from the Table 3.11, 52.25% (27.75% + 24.5%) Int. /year of the interruption frequency are due the short circuit (both temporary and permanent), 33.38% is due to operation, and 14.36% due to earth fault.

Table 3.12 Percentage of outages in terms of duration over two years

	DPEF	DPSC	DTEF	DTSC	OP
% duration	14.6	37.484	7.85	10.763	29.31

According to Table 3.12, 48.24% (hr. /year) of the interruption duration is due the short circuit, 29.3% is due to operation, and 22.45% due to earth fault.

3.3. Solar Power Resource Assessment

Before installing a solar panel at a specific location, it is advisable to investigate the viability of solar power-based DG installation on the selected area. PV cells must be able to produce energy during the hours of sunlight and solar irradiation. Therefore, daylight hour was taken into account during design and according to [32], it has to be between 4-6 Kwh/m²/day. The national meteorology Agency of Ethiopia records the Guder site's sunshine hour, and the data obtained is tabulated in Table 3.13 given below.

Table 3.13 Monthly average sunshine data of Guder site (National Meteorology Agency)

Year	**Month**											
	Jan	**Feb**	**Mar**	**Apr**	**May**	**Jun**	**Jul**	**Aug**	**Sep**	**Oct**	**Nov**	**Dec**
2016	11.5	8.8	7.5	6.4	6.5	4.7	3.9	3.6	5.1	8.4	9.1	8.2
2017	10.5	7.9	8.1	7.5	5.8	4.6	3.7	3.8	4.5	8.2	8.9	8.9
2018	10.8	8.2	7.6	6.9	8.2	5.2	4.2	4.2	6.5	7.8	7.9	9.9
2019	10.2	9	7.9	7.6	8.4	4.8	3.9	3.9	4.1	8.7	8.1	7.5

2020	10.6	8	7.6	6.9	6.4	5.3	3.8	4.1	4.9	8.8	9.7	9.9
2021	10.3	8.3	8.4	6.5	7.4	6.1	4.6	4.3	4.7	8.5	8.7	9.8
2022	10.5	8.8	8.6	7.2	7.3	5.8	5.1	4.7	5.2	8.9	9.5	9.7
Aver.	10.62	8.43	7.95	7.26	7.14	5.21	4.17	4.1	5.18	8.47	8.84	9.13

According to Table 3.13 above, the monthly average sunshine hour is sufficient for solar power design. The monthly solar radiation of the site is determined using a variety of methods. Among those several models, the Angstrom-Prescott estimating model is the most commonly used and preferable method [32]. The original regression formula for the Angstrom-Prescott type, which considers the daily radiation averaged over a month to clear day radiation in a specific place and the average proportion of potential hours of sunshine is given in equation (2.21)below:

$$\frac{H}{Ho} = a + b(\frac{S}{So}) \tag{3.12}$$

Where, H -is the daily average global radiation on the horizontal surface in (Kwh/m² /day), HO-average monthly extraterrestrial radiation of the horizontal surface (Kwh/m² /day), S-average monthly daily sunshine hour. So - average daily length for the month, and ‘a’ and ‘b’ are the Angstrom constants. Equation 3.13 below used to compute the average daily extraterrestrial radiation of the horizontal surface (HO).

$$Ho = \left(\frac{24}{\pi}\right) Isc \left[1 + 0.033 Cos\left(\frac{360n}{365}\right)\right] * [Cos\varphi \mathrm{Cos}\delta \mathrm{Sin}\omega s + (\frac{2\pi\omega s}{360}) Sin\varphi \mathrm{Sin}\delta \tag{3.13}$$

Where, Isc- solar constant having 1367 W/m^2, φ- is selected site latitude, δ- solar declination, ωs - average sunrise hour angle for the given month, and n- is the number of days of the year starting from January. The solar declination (δ) and average sunrise hour angle (ωs) can be calculated by equation (3.14) and (3.15) respectively [32]:

$$\delta = 23.45 Sin\left(360 \frac{284 + n}{365}\right) \tag{3.14}$$

$$\omega s = Cos^{-1}(-tan\varphi tan\delta) \tag{3.15}$$

The maximum possible sunshine duration (So) can be obtained by using the equation (3.16) given below:

$$So = \frac{12}{15}\,\omega s \tag{3.16}$$

The Angstrom constants has been obtained from the relationship given as in equation (3.17) and (3.18) [32]:

$$a = -0.11 + 0.235Cos\varphi + 0.323(\frac{S}{S0}) \tag{3.17}$$

$$b = 1.449 - 0.553Cos\varphi - 0.694(\frac{S}{S0}) \tag{3.18}$$

By having the above relation, the solar radiation of Guder site is calculated, and tabulated as in Table (3.16).

Let, be start the calculation for January, which has an average sunshine hour value of 10.62; from equation (3.12), $\frac{H}{Ho} = a + b(\frac{S}{So})$.

Where, $Ho = \left(\frac{24}{\pi}\right) Isc\ \left[1 + 0.033Cos\left(\frac{360n}{365}\right)\right] * [Cos\varphi \mathrm{Cos}\delta \mathrm{Sin}\omega s + (\frac{2\pi\omega s}{360})Sin\varphi \mathrm{Sin}\delta$.Then, first $\omega s,$ and δ value must be determined. Therefore, from equation (3.14), and (3.15) we have$\delta = 23.45Sin\left(360\,\frac{284+n}{365}\right)$, and $\omega s = Cos^{-1}(-tan\varphi tan\delta)$. By using these given formulas, we can calculate the $\delta,$ and ωs values as follow;

$\delta = 23.45Sin\left(360\,\frac{284+n}{365}\right)$ = 23.4Sin (360 $\frac{284+365}{365}$) = -23.086

$\omega s = Cos^{-1}(-tan\varphi tan\delta)$= $\omega s = Cos^{-1}(-\tan(8.98)\tan(-23.086))$= 89.9

And from equation (3.16),

$So = \frac{12}{15}\omega s$. $Hence, So = \frac{12}{15}$(89.9)= 12 Therefore,

$Ho = \left(\frac{24}{3.14}\right) 1367\ \left[1 + 0.033Cos\left(\frac{360*365}{365}\right)\right] * [Cos(8.98)\mathrm{Cos}(-23.086)\mathrm{Sin}(89.9) + \left(\frac{2*3.14*89.9}{360}\right)Sin(89.9)\mathrm{Sin}(-23.086)]$ = 9,929.75Wh/m2

From equation (3.17) and (3.18), the regression coefficients ‘’a ‘’and ‘’b’’ has been obtained as follow;

$a = -0.11 + 0.235Cos\varphi + 0.323(\frac{S}{S0})$

$a = -0.11 + 0.235Cos(8.98) + 0.323(\frac{S}{S0}) = 0.125 + 0.323(\frac{S}{S0})$

$b = 1.449 - 0.553Cos\varphi - 0.694(\frac{S}{S0})$

$b = 1.449 - 0.553Cos(8.98) - 0.694\left(\frac{S}{S0}\right) = 0.896 - 0.694(\frac{S}{S0})$

From equation (3.12), we have $\frac{H}{Ho} = a + b(\frac{S}{So})$. Therefore, from this equation we can drive for H. Then, $H = Ho(a + b\left(\frac{S}{So}\right))$. No we have Ho, a, b, S, and So values, by simple substitution we can obtained H value.

$H = 9{,}929.75[(0.125 + 0.323\left(\frac{10.62}{12}\right)) + (0.896 - 0.694\left(\frac{10.62}{12}\right))\left(\frac{10.62}{12}\right)]$ = 6,547.69 Wh/m^2 = 6.55 Kwh/m^2/day**.** By, following the same formula, and procedure, the overall solar radiation of site Guder has obtained, and organized in Table (3.14) below.

Table 3.14: Monthly average daily solar radiation of Guder site for seven years (2016-2022)

Av. Solar radiation in (Kwh/m^2/day)	**Month**											
	Jan	Feb	Mar	Apr	May	Jun	Jul	Aug	Sep	Oct	Nov	Dec
	6.55	6.34	6.23	6.04	6.01	5.19	4.63	4.56	5.17	6.4	6.46	6.5

The performance of the solar panel is determined by the average monthly daily solar radiation. The solar irradiation measured exists within the estimated range of 4.56-6.55 kwh/m^2/day. The solar radiation of the Guder location shows that it has sufficient potential solar energy resources, even when compared to developed countries that utilize more renewable energy sources.

3.4. Reliability Indices Comparison with Benchmark Standards

In Table 3.15 shown below, the fundamental reliability indices of SAIDI, SAIFI, and ASAI for nine developed countries are considered as a benchmark. The average values for SAIFI, SAIDI, and ASAI in the reliability evaluation of the Guder distribution substation are 355, 336.945 and 96.2 percent, respectively. Better reliability performance has fewer outages or outages for a shorter amount of time which is indicated by a lower number of the SAIDI, SAIFI, and ASAI indices. Poorer performance is indicated by higher SAIDI and SAIFI index numbers. When benchmarks are compared to the average SAIDI and SAIFI value of the Guder distribution substation, poorer performance is observed.

Table 3.15: Standard bench marking reliability indices (Bewketu Getie, 2020)

Developed Country	SAIFI (int./cust./yr.)	SAIDI (hr./cus./yr.)	ASAI (%)
USA	1.5	4	99.91
France	1	1.03	99.97
Germany	0.5	0.383	99.99
Austria	0.9	1.2	99.97
Denmark	0.5	0.4	99.98
UK	0.8	1.5	99.96
Italy	2.2	0.967	99.99
Spain	2.2	1.733	99.96
Netherland	0.3	0.55	99.97
Ethiopia	20	25	99.425

The reliability of Guder distribution substation is not good enough as compared to standard benchmarks. Even so, it performs worse than Ethiopia's typical benchmark value.

3.5. Load Flow Analysis of Radial Distribution System

The operation, control, and planning of power systems now extensive use of efficient and reliable load flow solution techniques as Gauss-Seidel (G S), Newton Rapson (N-R), and fast decoupled load flow. However, it has been repeatedly demonstrated that these techniques may become ineffective when used to analyze distribution systems because of the unique characteristics of such networks, including radial structure, high resistance-reactance(R/X) ratio, un-transposed lines, unbalanced loads, and single-phase and two-phase laterals.

In addition to these issues, distribution network matrices are typically unreliable, which could lead to numerical issues with the traditional power flow algorithm. Methods created to fix radial distribution networks with poor conditions can be categorized into two groups. The first category of methods includes N-R and G-S. The second set of approaches, on the other hand, are based on forward and/or backward sweep processes that employ Kirchhoff's principles or the well-known bi-quadratic equation[33]. The forward and/or backward sweep load flow approach is used in this work.

3.5.1. Forward and Backward Sweep Load Flow

The majorities of backward/forward sweep-based power flow algorithms uses the radial network topology and are made up of either forward or backward sweep operations. The backward sweep is essentially the branch current and/or power summing from the far end to the sending end of the feeder and laterals, whereas the forward sweep is mostly the node voltage calculation from the sending end to the far end of the feeder and laterals. Some algorithms also compute the node voltages in backward sweeps in addition to the branch current and/or power summing.

3.5.2. Forward Backward Sweep Load Flow Algorithm

Both the branch current to bus voltage matrix (BCBV) and the bus injection to branch current matrix (BIBC) are two derived matrices that are used to build the forward and backward sweep algorithms. The corresponding current-injection-based model is more useful for distribution networks[34].

Step One: Backward sweep

Branch currents from loads to system are collected for each iteration k. The bus-injection to branch-current (BIBC), which connects the bus-injected current to the branch current, must first be determined in order to determine the branch current. The ith bus's current injection's kth iteration is,

$$\mathrm{Ii}^{k} = \mathrm{Ii}^{r}(\mathrm{vi}^{k}) + j\mathrm{Ii}^{i}(\mathrm{vi}^{k}) = (\frac{Pi + jQi}{vi^{k}}) + \cdots \tag{3.19}$$

Where $\mathrm{vi}^{k}$and $\mathrm{Ii}^{k}$are the bus voltage and current injection of the i^{th}bus at the k^{th}iteration respectively.

Ii^{r} And Ii^{i} are real and imaginary parts of the current injection of bus i at the k^{th} iteration, respectively.

Development of Relationship Matrix

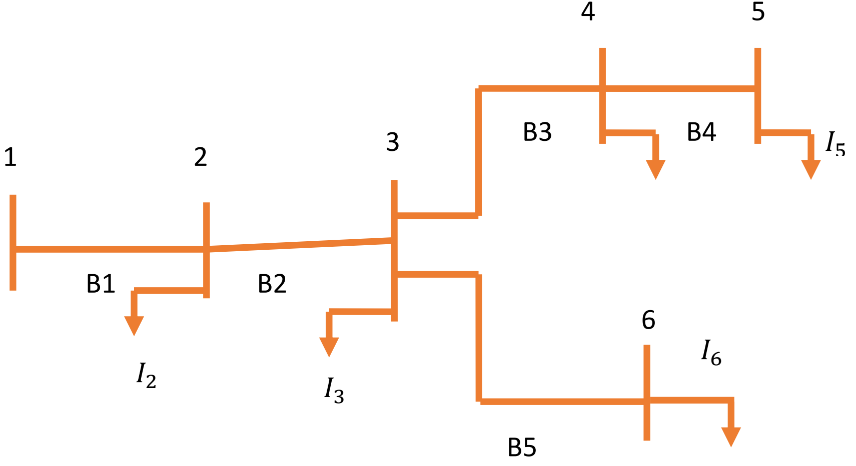

Figure 3.5: Sample distribution system[33]

Branch currents are calculated by applying Kirchhoff's current law (KCL) to the given network[33]. Here simple radial distribution system network was considered as an example. From a given example here, the branch currents of B1, B2, B3, B4, and B5 can be expressed as defined in the below equations.

$$B_1 = I_2 + I_3 + I_4 + I_5 + I_6 \tag{3.20}$$

$$B_2 = I_3 + I_4 + I_5 + I_6 \tag{3.21}$$

$$B_3 = I_4 + I_5 \tag{3.22}$$

$$B_4 = I_5 \tag{3.23}$$

$$B_5 = I_6 \tag{3.24}$$

Consequently, the following is an expression of the relationship between bus current injections and branch currents:

$$\begin{bmatrix} B_1 \\ B_2 \\ B_3 \\ B_4 \\ B_5 \end{bmatrix} = \begin{bmatrix} 1 & 1 & 1 & 1 & 1 \\ 0 & 1 & 1 & 1 & 1 \\ 0 & 0 & 1 & 1 & 0 \\ 0 & 0 & 0 & 1 & 0 \\ 0 & 0 & 0 & 0 & 1 \end{bmatrix} \begin{bmatrix} I_2 \\ I_3 \\ I_4 \\ I_5 \\ I_6 \end{bmatrix} \tag{3.25}$$

The above equation (3.25) can be expressed as,

$$[B] = [BIBC]\ [I] \tag{3.26}$$

Where: BIBC is a bus injection to branch the current matrix

Step two: Forward sweep

From Figure 3.5 illustrated above, the link between branch currents and bus voltages is expressed as follows.

$$\mathrm{V}_2 = \mathrm{V}_1 - (\mathrm{Z}_{12}\mathrm{B}_1) \tag{3.27}$$

$$\mathrm{V}_3 = \mathrm{V}_1 - (\mathrm{Z}_{12}\mathrm{B}_1 - \mathrm{Z}_{23}\mathrm{B}_2) \tag{3.28}$$

$$\mathrm{V}_4 = \mathrm{V}_1 - (\mathrm{Z}_{12}\mathrm{B}_1 - \mathrm{Z}_{23}\mathrm{B}_2 - \mathrm{Z}_{34}\mathrm{B}_3) \tag{3.29}$$

$$\mathrm{V}_5 = \mathrm{V}_1 - (\mathrm{Z}_{12}\mathrm{B}_1 - \mathrm{Z}_{23}\mathrm{B}_2 - \mathrm{Z}_{34}\mathrm{B}_3 - \mathrm{Z}_{45}\mathrm{B}_5) \tag{3.30}$$

$$\mathrm{V}_6 = \mathrm{V}_1 - (\mathrm{Z}_{12}\mathrm{B}_1 - \mathrm{Z}_{23}\mathrm{B}_2 - \mathrm{Z}_{56}\mathrm{B}_5) \tag{3.31}$$

Where, Zij- the line impedance between bus i and j and Vi- is the voltage at bus i. Other buses can be operated in a similar manner, therefore the relationship between branch currents and bus voltages can be defined as follows:

$$\begin{bmatrix}\mathrm{V}_2\\\mathrm{V}_3\\\mathrm{V}_4\\\mathrm{V}_5\\\mathrm{V}_6\end{bmatrix} = \begin{bmatrix}\mathrm{V}_1\\\mathrm{V}_1\\\mathrm{V}_1\\\mathrm{V}_1\\\mathrm{V}_1\end{bmatrix} - \begin{bmatrix}\mathrm{Z}_{12} & 0 & 0 & 0 & 0\\ \mathrm{Z}_{12} & \mathrm{Z}_{23} & 0 & 0 & 0\\ \mathrm{Z}_{12} & \mathrm{Z}_{23} & \mathrm{Z}_{34} & 0 & 0\\ \mathrm{Z}_{12} & \mathrm{Z}_{23} & \mathrm{Z}_{34} & \mathrm{Z}_{45} & 0\\ \mathrm{Z}_{12} & \mathrm{Z}_{23} & 0 & 0 & \mathrm{Z}_{56}\end{bmatrix}\begin{bmatrix}\mathrm{B}_1\\\mathrm{B}_2\\\mathrm{B}_3\\\mathrm{B}_4\\\mathrm{B}_5\end{bmatrix} \tag{3.32}$$

In general, equation (*2.21*) above can be expressed as follows:

$$\mathrm{V}^{k+1} = [\mathrm{V}_1] - [BCBV][B] \tag{3.33}$$

3.5.3. Formulation of the BIBC and BCBV Matrix

Branch currents and bus current injections are related, as shown by the BIBC matrix. The BIBC matrix can immediately calculate the corresponding variations at branch currents that are produced by variations at bus current injections. Branch currents and bus voltages are represented by a matrix called the BCBV matrix. The BCBV matrix can directly compute the corresponding fluctuations at bus voltages, which are caused by variations at branch currents. The following steps are what must be taken in order to form the BIBC and BCBV.

Procedure 1: BIBC Formation:

The equation formulated below can be used to convert the power injections at each node into comparable current injections, and by applying Kirchhoff's Current Law (KCL) at each node, a series of comparisons can be created. Now, the network's branch currents may all be sculpted as a function of the corresponding current injections [35].

$$\mathrm{Iii}^{iter} = \mathrm{Iii}^{r}\left(\mathrm{vii}^{iter}\right) + j\mathrm{Iii}^{ii}\left(\mathrm{vi}^{iter}\right) = \left(\frac{PS(ii) - jQS(ii)}{vii^{iter}}\right)^{*} \tag{3.34}$$

Equivalent current injection for the load flow solution is as shown in the equation above for the iter-th iteration at the ii-th node.

$$[\mathrm{I_B}] = [BIBC][I] \tag{3.35}$$

For a general network, the following steps could be used to shape the BIBC matrix.

Step 1: The BIBC matrix's dimension is m x (n-1) for a distribution system having n-bus and m-branch section.

Step 2: : If a line section (Bk) is located between bus i and bus j, copy the column of the ith bus of the BIBC matrix to the column of the jth bus and fill a 1 to the position of the k-th row and the j-th bus column.

Step 3: Repeat steps 2 until the BIBC matrix contains all of the network's branches.

Procedure 2: BCBV formulation:

The relationship between branch current and node voltages is defined by the Branch-Current to Node Voltage (BCBV) matrix. Kirchhoff's Voltage Law (KVL) can be used to quickly determine the relationships between the branch currents and node voltages. The general form can be represented as:

$$[\Delta V] = [BCBV]\ [IB] \tag{3.36}$$

Where BCBV=ZB*BIBC*$\overline{IB}$, ZB=diagonal impedance

For a universal network, the following steps can be used to create the BCBV matrix:

Step 1: The BCB matrix's dimension for a distribution system with m branch sections and n buses is (n-1) x m.

Step 2: If a line section is located between bus i and bus j, copy the row of the ith bus of the BCBV matrix to the column of the jth bus and fill the line impedance (Zij) to the position of the kth column and the jth bus row.

Step 3: Steps 2 should be repeated until all network branches are represented in the BCBV matrix.

3.6. Incorporation of DG into Load Flow

Assume that a single source radial distribution network with NL branches, a DG source connecting to node i will be installed at node i. Although it is well known that the DG provides active power (PGi^{DG}) and reactive power(QGi^{DG}) is dependent on the DG's source and can either be provided to or consumed by the systems. This active and reactive power causes an active current (IDGi^{r}) and a reactive current (IDGi^{i}) to flow through the system, changing the active and reactive components of the branch current set α. At the i^{th} node, the total apparent power is:

$$S = \mathrm{SD_i} = \sum \mathrm{pD_i} + j\mathrm{QD_i} \quad \mathrm{i}=1, 2, 3, \ldots\mathrm{NB} \tag{3.37}$$

Current at $i\,th$ node:

$$ID = \mathrm{I}^{wth\ out\_DG}\ D\_i = \left(\frac{SD\_i}{Vi}\right)^{*} \tag{3.38}$$

The active and reactive power demand at the i^{th} node, where a DG unit is installed must be modified in order to take the DG model into account.

$$\mathrm{P}^{with\ \_DG}\ D_i \quad = \quad \mathrm{P}^{with\ out_{DG}}\ D_i \ - \ \mathrm{PGi}^{DG} \tag{3.39}$$

$$\mathrm{Q}^{with\ \_DG}\ D_i \quad = \quad \mathrm{Q}^{with\ out_{DG}}\ D_i \mp \ \mathrm{QGi}^{D\ G} \tag{3.40}$$

DG power at i^{th} node:

$$SD_i = \sum \quad {PG_i}^{DG} \pm {QG_i}^{DG} \qquad \mathrm{i}= 1, 2, 3 \ldots\ldots\mathrm{NB} \tag{3.41}$$

i^{th} Node total new apparent power:

$$S = SD_i - SDG\_i \tag{3.42}$$

New current at the i^{th} node:

$$ID = I^{with\_DG} \, D\_i = \left(\frac{SD\_i \;\; SDG\_i}{Vi}\right)^* \tag{3.43}$$

The updated network power can be stated in matrix form as follow:

$$[S] = [SD\_i] - [SDG\_i] \tag{3.44}$$

3.7. Distribution Networks Load Flow with DG Algorithm

A list of algorithmic steps for distribution networks power flow is discussed below:

Step one: Read line and bus data of distribution networks.

Step two: Determine each node's DG power and update the system bus information.

Step three: Determine the overall power demand with DG.

The relationships can be described as: $[S] = [SD\_i] - [SDG\_i]$

Step four: compute power flow solution of distribution networks.

A. Reducing power loss by using DG

The following explanation illustrates how DG decreases power loss in the radial distribution system using the optimal size and location.

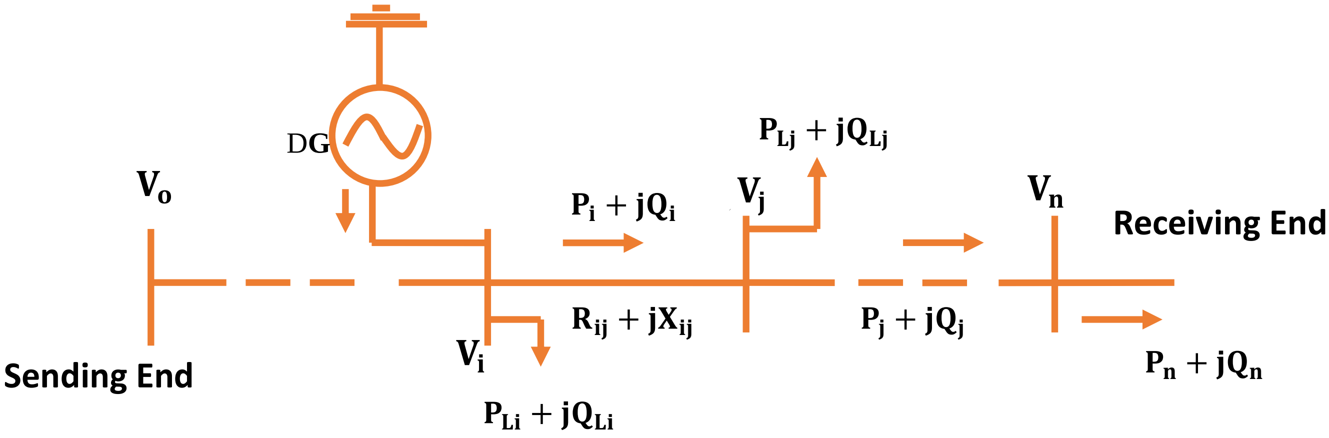

Figure 3.6: Radial distribution system with DG integration at bus i [36]

Given that DG injects real power P_{DG} at bus i is assumed that the load on this bus will deviated from P_{Li} to $(P_{Li} - P_{DG})$

With DG added on branch ij, mathematically active power loss is given by

$$\mathrm{P}_{\mathrm{Loss\ i,j}}^{\mathrm{DG}} = \frac{Ri,j}{vi^2}\left[(Pi - PDG)^2 + Qi^2\right] \tag{3.45}$$

After inserting the DG, each branch of power loss is provided by;

$$\mathrm{P}_{\mathrm{T\ loss}}^{\mathrm{DG}} = \sum_{i,j=1}^{n} \mathrm{P}_{\mathrm{Loss\ i,j}}^{\mathrm{DG}} \tag{3.46}$$

Power loss change ($\Delta\mathrm{P}_{\mathrm{loss}}^{\mathrm{DG}}$)with the integration of DG is calculated as expressed in equation below:

$$\Delta\mathrm{P}_{\mathrm{loss}}^{\mathrm{DG}} = \sum_{i,j=1}^{n} \mathrm{P}_{\mathrm{Loss\ i,j}} - \sum_{i,j=1}^{n} \mathrm{P}_{\mathrm{Loss\ i,j}}^{\mathrm{DG}} \tag{3.47}$$

3.8. Proposed Methods for DG placement and Sizing

The first condition has aimed to find the best optimal sizing and placement of DG by using PSO algorithm. The system is expected to fulfill a number of constraints that are part of the multi-objective function derives from a number of different objective functions in the power distribution system.

3.8.1. Particle Swarm Optimization (PSO)

The Particle Swarm Optimization (PSO) algorithm has a variation called Multi-Objective Particle Swarm Optimization that is specially made to address multi-objective optimization issues. The Pareto front is a collection of solutions that represents the trade-offs between various objectives, and it extends the conventional Multi-Objective Particle Swarm Optimization method by taking into account numerous competing purposes at once.

In PSO, to locate the Pareto-optimal solutions, a population of particles (possible solutions) flows around the search space. The program investigates the search space and moves closer to the Pareto front by repeatedly updating the positions and velocities of the particles.

3.8.1.1.Basic Particle Swarm Optimization

Each individual member of the PSO algorithm is referred to as "particle," and each particle moves around the multi-dimensional search space with a velocity that is continuously updated by the particle's experience as well as the experience of its neighbors or the swarm.

A basic PSO technique is straightforward because it just uses two model equations. In this case, each particle's coordinates stand for a potential resolution connected to vectors of position (Xi) and velocity (Vi). Every iteration step will see a change in each particle's velocity in the direction of its pbest and gbest values. The last position will then be added to the new velocity to determine each particle's new position. The next two equations are the two main ones.

$$\mathrm{Vi}(\mathrm{I}+1) = w * vi(I) + c1 * r1 * (pbi - xi) + c2 * r2 * (gbi - xi) \tag{3.48}$$

$$Xi(I+1) = xi(I) + vi(I+1) \tag{3.49}$$

Where:

Vi- velocity for the particle i,

W- Weight of inertia

I – iteration

c1& c2- acceleration coefficients with the range of [0, 4]

Pbi- the previous best particles' optimal position

Xi- is i th present position of particles

r1& r2- random variables with a range of [0, 1]

Gbi- optimum position within the particles' population

The following are the fundamental PSO techniques:

1. Particle X (I): - is a potential solution represented by a real-valued vector with D dimensions, where D is the total number of optimized parameters.
2. Population: - is the collection of x particles at time t.
3. Fitness Function: - is used to identify the ideal response. It is typically an objective function.
4. Swarm: - A population of moving particles that appears to be randomly moving has a tendency to group together.
5. Particle's velocity V (I): - is the vector which measures the velocity and direction of moving particles. It is represented by a real valued D-dimensional vector.
6. Velocity Update: The equation updates the velocity (I).
7. Update on Position: To locate the global optimum, each particle in PSO changes their positions.

8. Inertia weight w (I): This control parameter regulates how much the previously speed affects the speed of the moment.

9. Personal best (pbi): - As it progresses across the area of search, the particle compares its current position's fitness value to the best fitness value, and it has ever achieved at any point in the past. Every particle in the swarm has an individual best position, which can be identified and updated throughout the search process and is related to the best fitness achieved. In general, it is the particle's most advantageous place out of all those it has already visited.

10. Global best (gbi): - is the best position out of all the individual best spots that have been visited so far where the best fitness is obtained.

11. Stopping criteria: - are the conditions that will cause the search to come to an end.

3.8.1.2.Parameters of Particle Swarm Optimization

There are a few parameters in the basic PSO that need to be fixed. The basic PSO parameters are: Population (swarm) size Particle Velocity Random Numbers Iteration numbers Velocity Components Acceleration coefficients the population's size is the first factor. This is frequently established empirically based on the complexity and perceived difficulty of a problem. Values between 20 and 50 are very common. The second parameters in Equation (3.48), c1 and c2, are also known as acceleration coefficients because they govern the magnitude of random forces acting in the direction of gbi for b oth the personal best and the neighborhood best.

The values of c1 and c2 have a significant impact on how a PSO behaves. Every particle keeps going to move at their present speed until they collide with the search space boundary when c1=c2=0. On the other hand, all particles are independent when c1>0 and c2=0. When c1=0 and c2>0, all of the particles in the swarm are drawn to a single point, when c1=c2, all of the particles are drawn to the average of pbest and gbest, and when c1>c2. When c2>c1 then all particles are much more influenced by the global best position, which causes all particles to run prematurely to the optimal in all cases, the velocity update equation is changed, and each particle is more strongly influenced by its personal best position, leading to excessive wandering. However, the c1=c2=2.0 value was virtually always used in early PSO studies.

The PSO algorithm's iteration number is another crucial component for obtaining better results.

A search that is iterated to few times may end prematurely, Where as one that iterates too many times adds unnecessary computing complexity and demands more time.

3.8.1.3. PSO Implementation Steps

1. Problem formulation: Specify the optimization problem's constraints and objective functions. The goal of this situation is to reduce line losses in system while keeping in mind limitations like DG capacity limits, voltage limits, and network constraints.
2. Initialization: Set the parameters of the PSO algorithm, such as the population size, the variety of DG sizes, iterations, inertia weight, acceleration coefficients, and locations, to their initial values.
3. Particle Initializing: Each particle in this population represents a potential solution. Give the particles within the boundaries random placements and velocities.
4. Assess Fitness: Assess the fitness of each particle by computing the distribution system's power losses for the relevant DG sizes and locations.
5. Update Personal Best: Based on every particle's current dominance and fitness, update the personal (Pbest) best position for that particle.
6. Update Global Best: Update the Gbest by locating the non-dominated solutions among all particles.
7. Update Velocities and Positions: Update the particle's velocities and positions in accordance with their present velocities, positions, PBest, and GBest. To update the particle locations and speeds, use the PSO equations.
8. Boundary Constraint Handling: Use boundary constraint handling strategies to make sure that the particle positions stay within the acceptable range of DG sizes and locations.
9. Evaluate Convergence: Look for criteria for convergence, such as the maximum number of iterations or a suitable level of convergence.
10. Continue step 4 to 9 until the convergence requirements are satisfied.
11. Output Analysis: After the algorithm converges, examine the Pareto-optimal results to determine how both power losses are traded off. These solutions show several DG location and sizing possibilities in the distribution system.

12. Choose the Best Solution: Depending on your tastes and requirements, choose the best option from the Pareto-Optimal Front that achieves the desired balance between active and reactive power losses.

3.8.1.4. Problem formulation

For the operator to decide on the capacity of the chosen distribution network, there are several performance-related parameters that must be taken into account. The objective function and constraints are included in the algorithm's problem formulation.

A. Objective Function:

The PSO algorithm's objective function seeks to reduce both power loss and voltage variation. The following is a definition of it:

I. Reduction of power loss

The goal of power loss reduction is to eliminate overall losses in the distribution system to a minimum. The total amount of power lost throughout all system branches and lines might be used to describe it. It can be modeled mathematically as:

f1 = ∑ (Pl) (for all lines), and ∑ (Ql) (for all lines) (3.50)

By adding each network branch losses, the overall power loss in a distribution network may be computed. The following is the power loss formula:

Total real power loss (PTL) = Σ (I_ij^2 * R_ij) (3.51)

Total reactive power loss (QTL) = Σ (I_ij^2 * X_ij) (3.52)

Where;

I_ij - is the current flowing through branch (line) ij.
R_ij- is branch resistance
X_ij - is branch reactance

B. Constraints

The PSO algorithm includes a number of constraints to guarantee that the solutions are feasible. These limitations frequently include DG power, voltage range, and size.

I. DG Size Constraint

The DG size constraint makes sure that the DG units' size or capacity is within a predetermined range. It can be stated as follows:

$DG\_min. \leq DG\_size \leq DG\_max.$

Where, D_min. and D_max show the minimum and maximum DG sizes, respectively.

II. Voltage Range Constraint

Bus voltages are kept within allowable bounds by the voltage range limitation. It can be stated as follows:

$V\_min. \leq V \leq V\_max.$

Where, V_min. and V_max indicate the minimum and maximum voltage limits, respectively.

3.8.1.5.Optimal DG size and location using PSO algorithm

Let's assume that DG unit is connected to bus k in a radial distribution network. The power flow equations can be expressed as:

$$P\_k = Pload\_k - Ploss\_k + Pdg\_k \tag{3.53}$$

$$Q\_k = Qload\_k - Qloss\_k + Qdg\_k \tag{3.54}$$

Where;

P_k and Q_k are the injected active and reactive powers at bus k, respectively.

Pload_k and Qload_k are the active and reactive loads at bus k, respectively.

Ploss_k and Qloss_k are the active and reactive power losses at bus k, respectively.

P_dg_k and Qdg_k are the active and reactive power injected by the DG unit at bus k, respectively.

The voltage drop equation can also be used to express voltage at the DG connection point.

$$V\_k = V\_src - I\_k * Z\_k \tag{3.55}$$

Where;

V_k -is the voltage at bus k

V_src- is the source voltage

I_k -is the current flowing through the lines

Z_k -is the impedance of the line

The following steps can be accomplished objectively by using PSO technique to address the DG placement and size issue:

Step1: Load case information: The system data, including the generator data, bus data, and branch data, are saved in Matlab m-file.

Step 2: Determine the voltages at each node and the overall power loss in the distribution network at the initial condition.

Step3: Initialize the Swarm parameters:- Establish the limits of the DG size PDGrmax and PDGrmin as well as the velocity Vmax and Vmin.- Indicate the values of the acceleration coefficients c1 and c2 as well as the inertial weight w.- Assign the initial velocity and position (X_i = [X_{i1}, X_{i2},..., X_{in}], and Vi = [V_{i1}, V_{i2},..., V_{in}]).- Generate a random initial population of N particles with a D-dimensional search space.

Step 4: Obtain the fitness function's value and store the Pbest and Gbest values.

Step 5: Update the position and speed of a particle.

Step 6: Using the most recent particle position and velocity, determine the new fitness value of the fitness function for the entire particle. - For each particle's new position, new fitness values are computed. If a particle's new fitness value is higher than its previous Pbest value, the particle's Pbest value is changed to reflect the improved fitness value.

Step7: Update the Gbest and new Pbest. Each particle provides the ideal DG sizes and positions, as well as the related fitness value, which represents the least amount of power loss.

Step 8: Carry out the previously described process, beginning with step 5, as many times as is physically possible before printing the target problems best solution.

3.8.1.6.Procedure for applying PSO algorithm

1. Set the initial values for the population size, iterations, inertia weight, acceleration coefficients, and range of DG sizes and locations in the PSO algorithm (determining the initial values for the population size, iterations, inertia weight, acceleration coefficients, and range of DG sizes and locations in the PSO algorithm requires careful consideration and may vary based on the specific problem and domain. For instance, a common practice to set the population size is between 20 and 100, depending on the complexity of the problem).

2. Create a population of particles with each particle standing in for a potential solution. Within the boundaries, give the particles random placements and speeds.

3. Determine the voltage drop and power loss in the distribution system for the respective DG sizes and positions in order to assess each particle's fitness. Power loss reduction and voltage deviation control are both taken into account by the fitness function.

4. Based on the fitness and dominance of each particle, update the $\mathrm{P_{best}}$for that particle. In the search space, every particle keeps its optimal position.

5. Update $\mathrm{G_{best}}$position by figuring out which particles have non-dominated solutions. Power loss reduction and voltage deviation management are balanced by the Pareto-optimal front, which is represented by the GBest.

6. Adjust the particle's velocities and positions in accordance with their present positions, velocities, PBest, and GBest. Update the particle locations and velocities using the PSO equations while taking the DG size, voltage range, and power limitations into account.

7. Use boundary constraint management strategies to make sure the particle positions stay within the range of DG sizes and locations that are practical.

8. Look for convergence requirements, such as the maximum number of iterations or an acceptable degree of convergence. Repeat steps 3 to7 if the convergence conditions are not satisfied.

9. After the algorithm converges, examine the generated Pareto-optimal solutions to determine how voltage deviation control and power loss reduction are traded off. These solutions show several DG location and sizing possibilities in the distribution system.

10. Based on your unique tastes and requirements, choose the best option from the Pareto-optimal front while keeping in mind the ideal balance between power loss reduction and voltage deviation management.

3.8.1.7.Flow Chart of Particle Swarm Optimization

A flowchart of the optimal placement and sizing of DG using the PSO algorithm is shown in Figure 3.7.

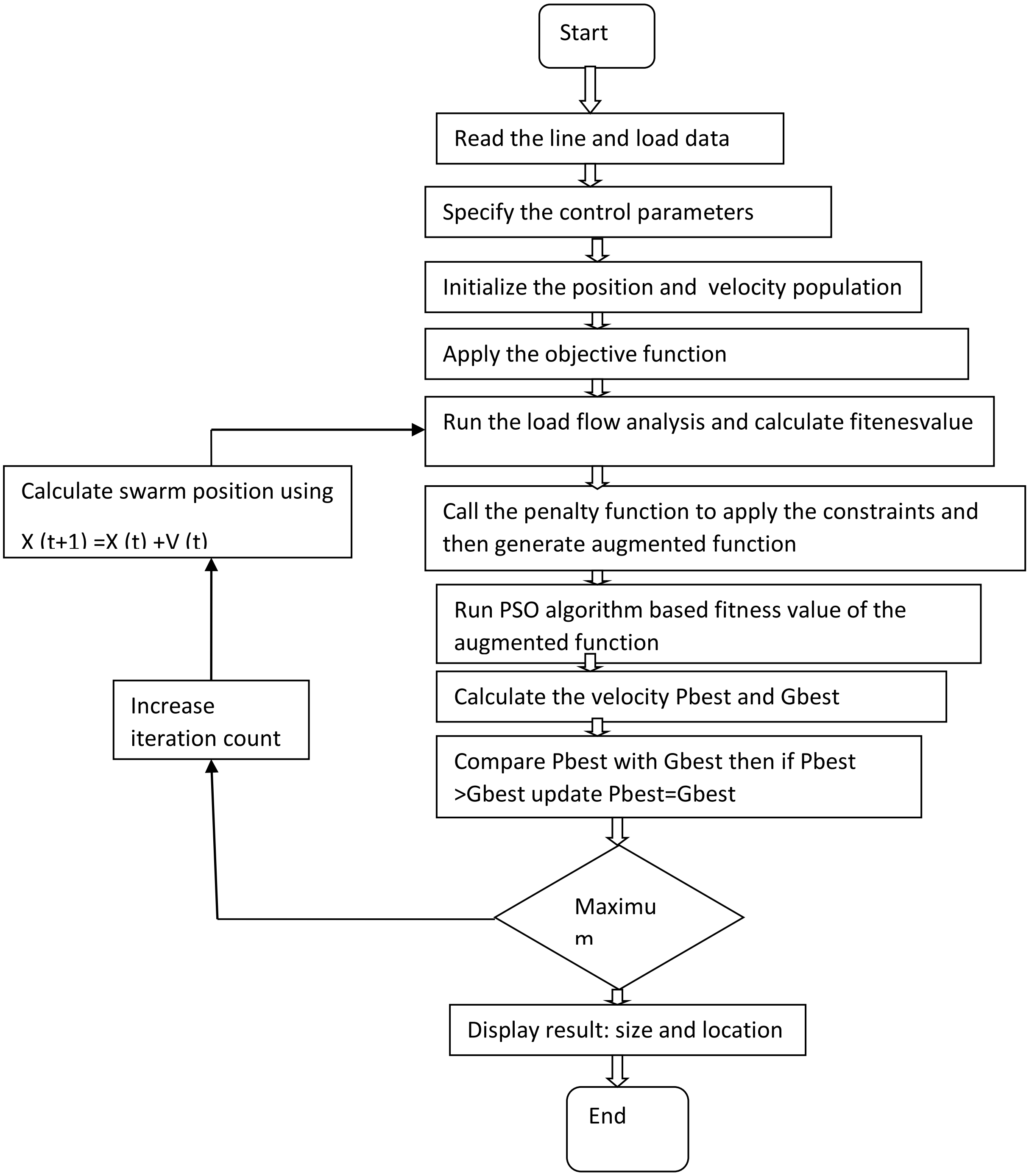

Figure 3.7 Flowchart of the proposed PSO

CHAPTER FOUR

4. RESULT ANALYSIS AND DISCUSSION

4.1. Introduction

This chapter explains how to model and simulate the existing system by using various DG sizes to raise the Guder town feeder's system reliability. The ETAP Software simulation has examined a variety of cases. The goal of the simulation is to assess how Distributed Generation (DG) affects the system's reliability and power loss. The Duration and Frequency outages are the two general categories of any distribution system reliability analysis. In this study, the frequency of interruption is significantly higher than the benchmark values, which should need mitigation techniques.

4.2. Introduction to ETAP Software

A completely graphical enterprise called Electrical Transient Analysis Program (ETAP) works with several Microsoft Windows operating systems (window 7, 8 and 10). For the purpose of constructing one-line diagrams, ETAP offers an intuitive, fully graphical user interface (GUI) that can be used to graphically add, delete, relocate, zoom in or out, turn on or off the grid, connect elements, change element size, change symbols, change the color of equipment and devices, make custom viewing themes, hide or show protective devices, set operating status, etc. ETAP is one of the well-integrated software for electrical systems, which gives engineers access to a variety of system presentations for various analysis and design needs. The program is used to examine various electrical analyses, including short circuit, reliability, load flow, arc flash, protection coordination, and others.

4.3. Reliability and Power Loss Evaluation with ETAP

ETAP software is one of the power system reliability analysis programs, as it was stated in the introduction part. Lines, transformers, loads, DG, external grid, bus bars, and other devices are among the ETAP equipment analyzed in this investigation. Failure rates and mean time to repair values for each component are needed in order to predict the reliability indices of the Guder town distribution system. The performance of the distribution system as a whole and the availability of individual lines are using reliability assessments including failure rate and mean time to repair.

Equations 4.1 and 4.2 can be used to compute the reliability indices of the existing substation[39].

$$\text{Failure rate}(\lambda) = \frac{\text{Number of outage of a system at agiven period}}{\text{Number of failures}} \tag{4.1}$$

$$\lambda = \frac{279.92}{323} + \frac{393.97}{387} = 0.8667 + 1.018 = 1.88 \text{ Failure/ yr.} \tag{4.2}$$

$$\text{Mean time to repair}(\text{MTTR}) = \frac{\text{Total Duration of outages}}{\text{Frequency of outag}es} \tag{4.3}$$

$$\text{MTTR} = \frac{(279.92+393.97)/2}{(323+387)/2} = \frac{336.945}{355} = 0.95 \ \text{hrs/int.} \tag{4.4}$$

The basic reliability parameters for reliability analysis are predicted by the ETAP software using the µA and MTTR equation. The failure rates of active and passive components are combined in ETAP to estimate a component's failure rate. The active failure rate is linked to the component failure mode that activates the primary protection zone around the failed component. It should be noted that only after repair or replacement could the failed component be put back in service. Electrical and failure inputs are present in all equipment. In a distribution system, for instance, a bus bar is provided inputs for its ratings, such as repair time, and failure inputs. Because EEU lacks such data, the failure rate and mean time to repair data are obtained from some reference papers and IEEE standards. Table 4.1 below shows the failure rates and repair times for various components including distribution transformers, and bus bars (IEEE Std C37.20.2-2015: IEEE Standard for Metal-Clad Switchgear, EPRI Technical Report[4]).

Table 4.1 Electrical equipment and failure inputs

Equipment Name	Failure rate (λ) (Failure/yr.)	Mean time to repair (MTTR) (Hr.)	Voltage level (KV)
Distribution transformer	0.015	200	15
Bus bar	0.001	2.00	15

4.3.1. Single Line Diagram of Guder Town Feeder

In this case single line diagram of the selected feeder is designed and labeled as “single line diagram “in figure 4.1.

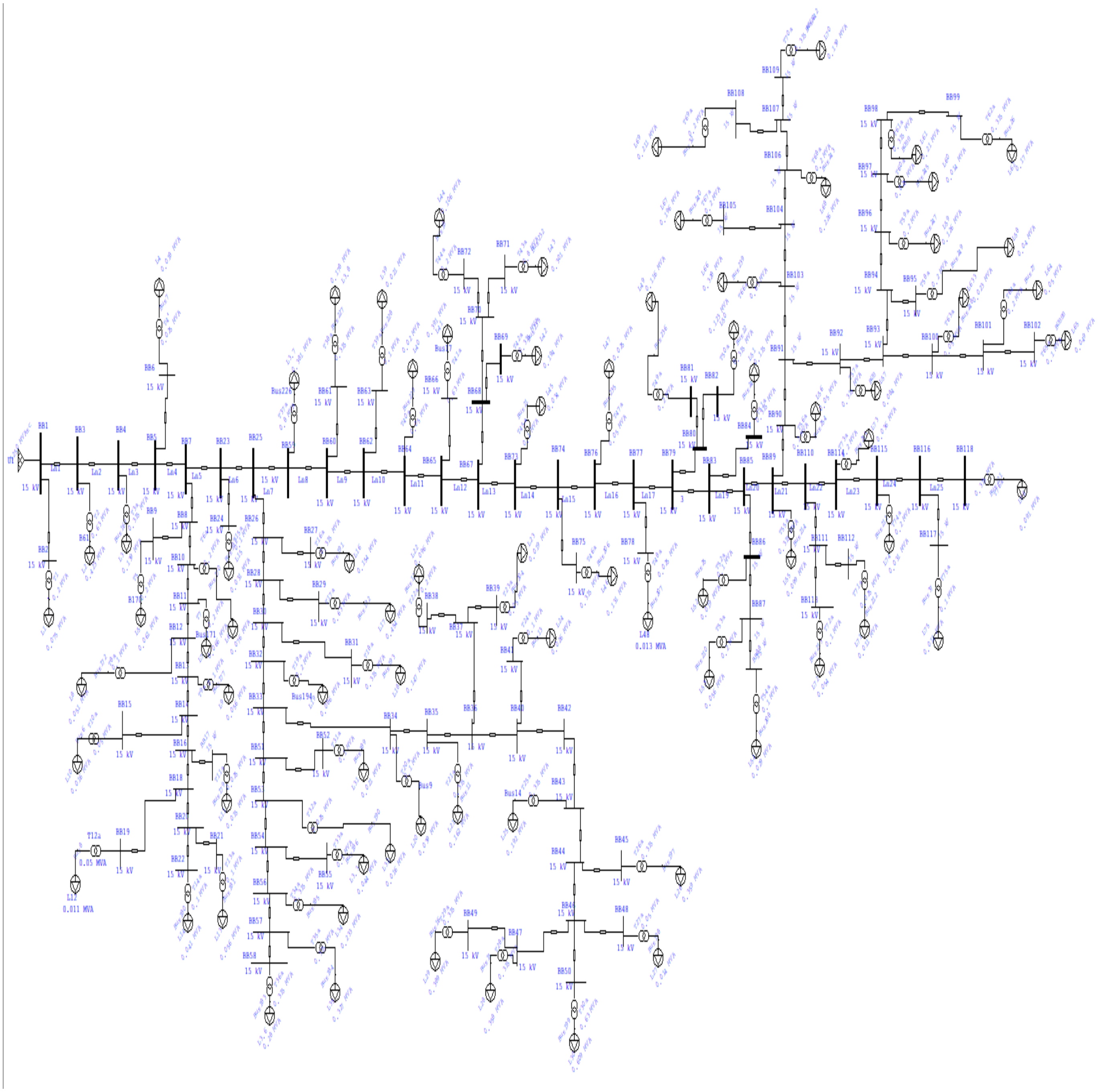

Figure 4.1: Existing system single-line diagram

In this study, three cases were considered for the reliability and power loss analysis. These are base case, and two different cases at optimal DG size and placement with the help of PSO algorithms.

Case1: Base case reliability and power loss analysis

The reliability indices of the existing system were shown in Table 4.2 below, and the single line diagram of the system for this scenario is discussed in figure 4.2.

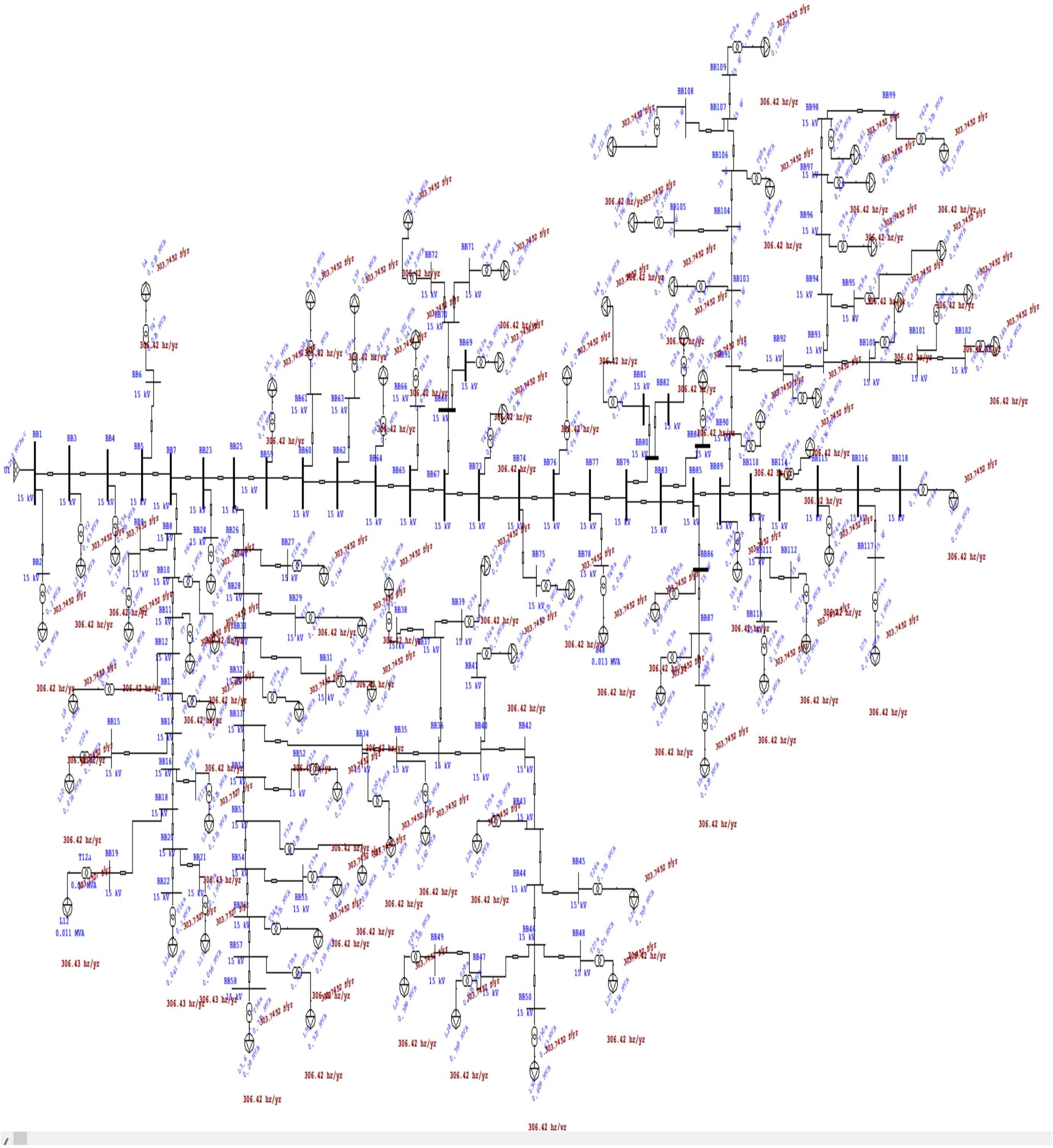

Figure 4.2: Single line diagram of Guder town feeder before DG penetration

Table 4.2: Base case reliability indices result before DG penetration

Project:	Msc;- Thesis	**ETAP 19.0.1**	Page:-	1
Location:	Guder		Date:	03-03-2024
Contract:	Case-1		SN:	
Engineer:	Firaol		Revision:	base
Filename:	Reliability Enhancement		Config.:	Normal

SUMMARY

System Indexes

AENS	31.1619 MW hr / customer.yr
ASAI	0.9650 pu
ASUI	0.03498 pu
CAIDI	1.374 hr / customer interruption
CTAIDI	68.433 hr / customer.yr
EENS	2368.307 MW hr / yr
SAIDI	306.4240 hr / customer.yr
SAIFI	303.7458 f / customer.yr

AENS	Average Energy Not Supplied
ASAI	Average service Availability Index
ASUI	Average Service Unavailability Index
CAIDI	Customer Average Interruption Duration Index
CTAIDI	System Customer Total Average Interruption Duration Index
EENS	Expected Energy Not Supplied
SAIDI	System Average Interruption Duration Index
SAIFI	System Average Interruption Frequency Index

Table 4.2 above illustrates the system reliability indices of the existing system. The current reliability indices for SAIFI, SAIDI, and EENS are recorded as 303.7458 fr/cust.yr,306.4240 hr/cust.yr, and 2368.307 MWhr/yr, respectively. These values exceed standard reliability indices, indicating a reliability issue within the existing system. Additionally, the feeder's real and reactive power losses for the existing system are measured at 611.9843 KW and 323.8237 KVar, respectively. This data highlights that the real and reactive power loss in the existing system are significant and require improvement.

Case 2: Reliability and power loss analysis when 2DGs penetrated at bus 97 and 111 with a capacity of 0.9615MW, and 0.9835MW respectively.

This scenario shows the results obtained by penetrating 2DGs to the network as indicated in single line diagram in figure 4.3 below.

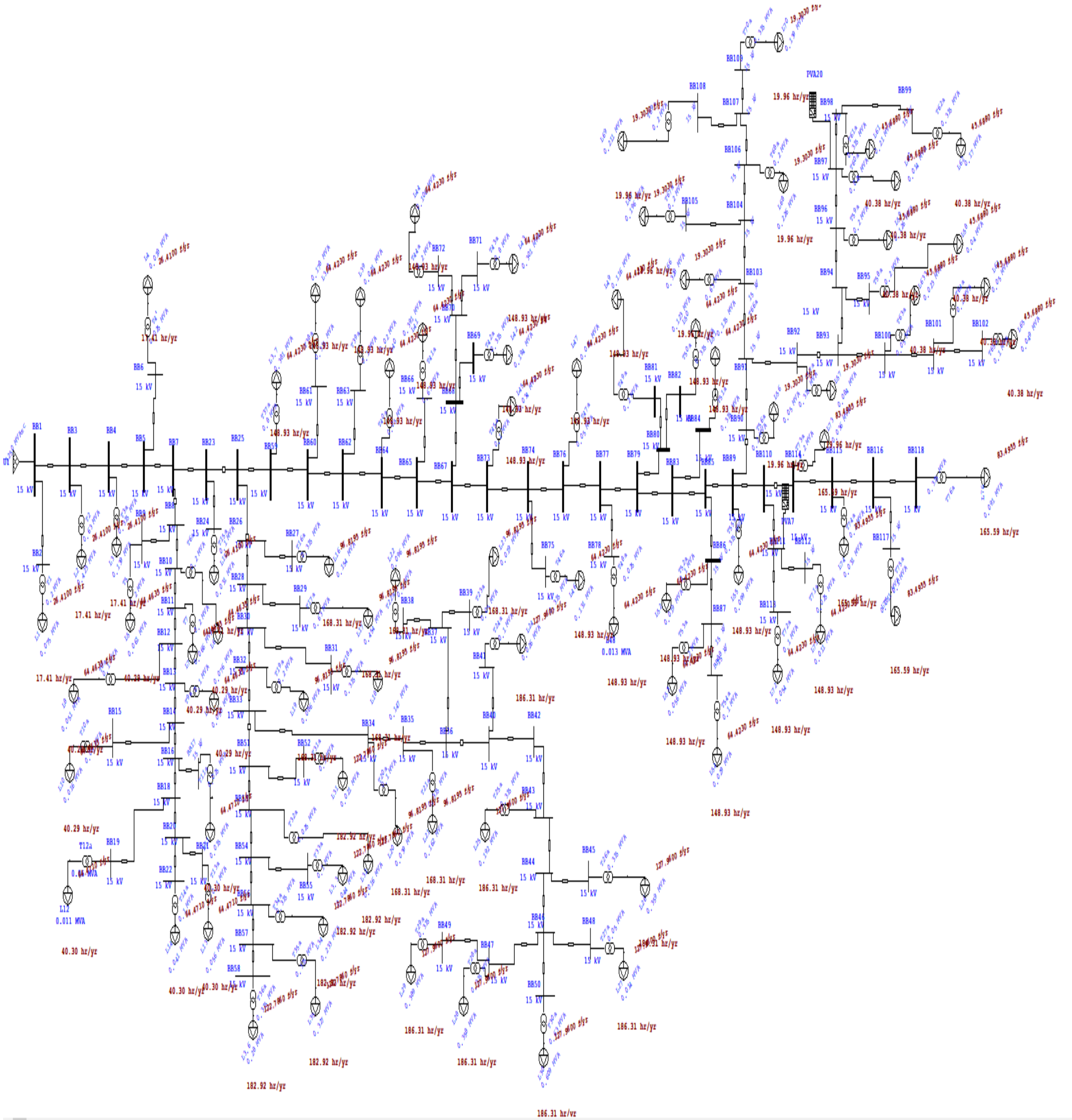

Figure 4.3: Single line diagram of the system with 2DGs penetration at bus 97, and 111

The summary results are also shown in Table 4.3 as follows.

Table 4.3: Reliability result for case-2

Project:	Msc;- Thesis	**ETAP 19.0.1**	Page:	-2
Location:	Guder		Date:	03-03-2024
Contract:	Case-2		SN:	
Engineer:	Firaol		Revision:	base
Filename:	Reliability Enhancement		Config.:	Normal

SUMMARY

System Indexes

AENS	12.5905 MW hr / customer.yr
ASAI	0.9872 pu
ASUI	0.01275 pu
CAIDI	1.581 hr / customer interruption
EENS	956.875 MW hr / yr
SAIDI	111.7216 hr / customer.yr
SAIFI	70.6736 f / customer.yr

AENS	Average Energy Not Supplied
ASAI	Average service Availability Index
ASUI	Average Service Unavailability Index
CAIDI	Customer Average Interruption Duration Index
EENS	Expected Energy Not Supplied
SAIDI	System Average Interruption Duration Index
SAIFI	System Average Interruption Frequency Index

Table 4.4 shows the overall reliability indices and power loss simulation results for case 2

Parameters	Base case	With 2DGs	Percentage enhancement (%)
Active power loss (KW)	611.9843	438.965	28.27
Reactive power loss(KVar)	323.8273	212.790	34.3
SAIFI (f/cust.yr)	303.7458	70.6336	76.74
SAIDI (hr/cust.yr)	306.4240	111.7216	63.54
EENS (MWh/yr.)	2368.307	956.875	59.6
DGs locations (bus)		97, and 111	
DGs size (MW)		0.9615, and 0.9835	

As observed, the values of the SAIFI, SAIDI, and EENS indices, previously recorded as 303.7458 fr/cust.yr,306.4240 hr/cust.yr, and 22368.307 MWhr/yr, respectively, have shown significant improvements. These indices have decreased to 70.6336fr/cust.yr, 111.7216 hr/cust.yr, and 956.875 MWhr/yr, respectively. This substantial reduction represents enhancement percentages of 76.74% for SAIFI, 63.54% for SAIDI, and 59.6% for EENS. Additionally, the real and reactive power losses have been notably reduced from 611.9843 KW and 323.8273 KVar to 438.965 KW and 212.79 KVar, respectively. This reduction translates to a decrease of 28.27% in real power loss and 34.3% in reactive power loss.

The improvements in system reliability indices and power losses signify the effectiveness of the proposed enhancements. The substantial decrease in SAIFI, SAIDI, and EENS indices demonstrates a remarkable enhancement in system reliability. Moreover, the notable reduction in real and reactive power losses reflects an improvement in the overall efficiency of the system. These results underscore the significance of the implemented measures in enhancing system performance and reliability, ultimately contributing to the optimization of power distribution operations.

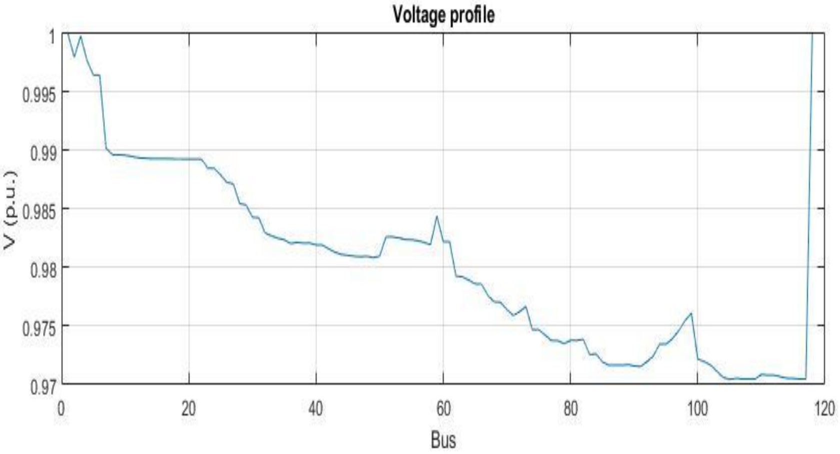

Figure 4.4: Voltage profile of the system after 2DGs penetrated at 114, and 131 buses

Case -4: Reliability and power loss result when 5DGs connected with a capacity of 1 MW each at bus 47, 53, 102, 111 and 132 respectively.

In this scenario, the impact of penetrating 5DGs to the existing system on reliability and power loss is observed and the implementation is shown in one line diagram in Figure 4.5 below and summary of the results obtained and discussed as shown in Table 4.5.

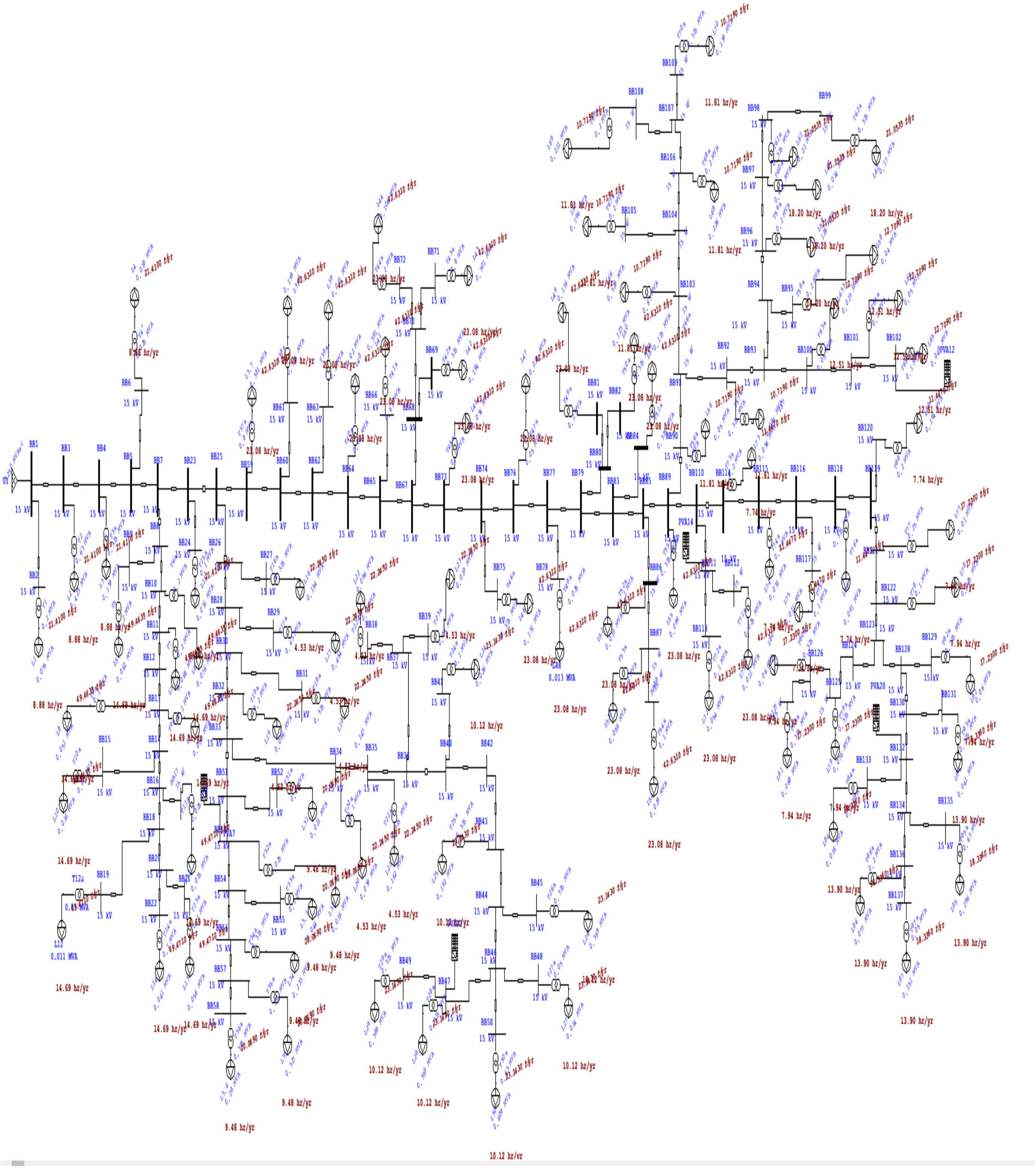

Figure 4.5: System network with integration of 5DGs at bus 47, 53, 102, 111, and 132

Table 4.5: Reliability results after 5DGs integrated to the system

Project: MSc Thesis	ETAP	Page: 3
Location: Guder	12.6.0H	Date: 12-02-2024
Contract: Case-3		SN: 03
Engineer: Fraol	Study Case: Case-03	Revision: Base
Filename: Reliability Improvement and power loss Reduction		Config.: Normal

SUMMARY

System Indexes

SAIFI	27.4968 f / customer.yr
SAIDI	13.6501 hr / customer.yr
CAIDI	0.496 hr / customer interruption
ASAI	0.9984 pu
ASUI	0.00156 pu
EENS	111.758 MW hr / yr
AENS	1.2700 MW hr / customer.yr

SAIFI	System Average Interruption Frequency Index
SAIDI	System Average Interruption Duration Index
CAIDI	Customer Average Interruption Duration Index
ASAI	Average service Availability Index
ASUI	Average Service Unavailability Index
EENS	Expected Energy Not Supplied
AENS	Average Energy Not Supplied

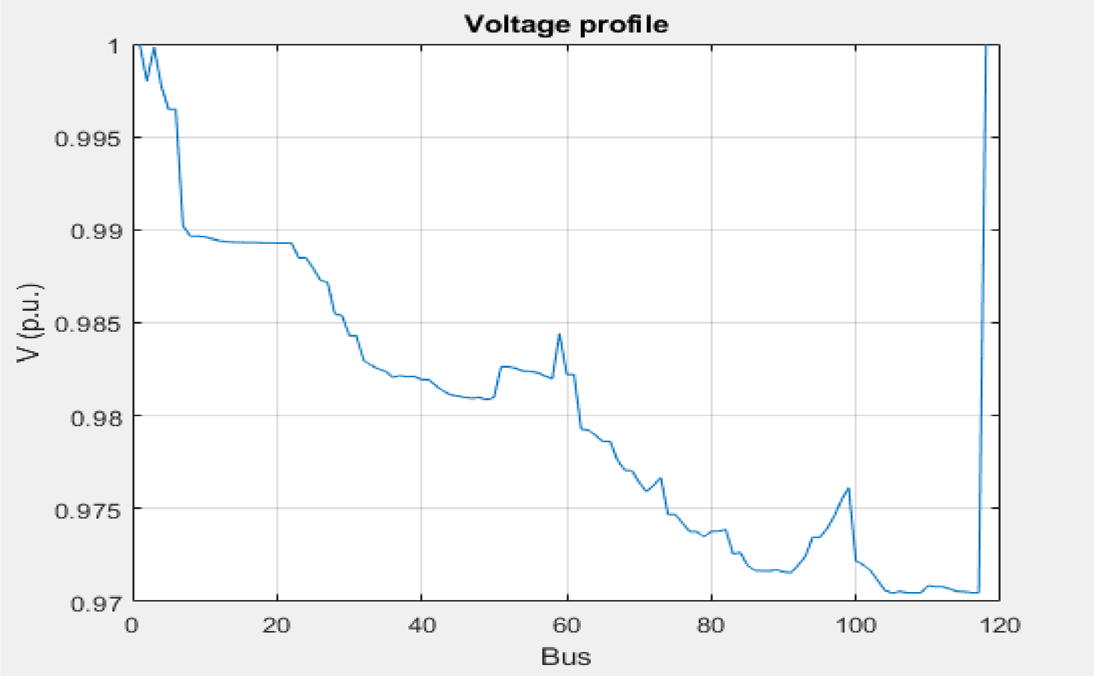

Figure 4.6 Voltage profile of the system for case-3

Table 4.6: Over all simulation result for case-3

Parameters	Base case	With 5DGs	Percentage enhancement (%)
Active power loss (KW)	611.9843	302.75	50.52
Reactive power loss(KVar)	323.8273	132.34	59.12
SAIFI (f/cust.yr)	303.7458	**27.4968**	91
SAIDI (hr/cust.yr)	306.4240	**13.6501**	95.54
EENS (MWh/yr.)	2368.307	111.758	95.28
DGs locations (bus)		47, 53, 102, 111and 132	
DGs size (MW)		1 at each	

As evident from the simulation results presented in the table 4.6 above, there has been a notable reduction in both active and reactive power losses. Specifically, the active power loss decreased by 50.52%, while the reactive power loss decreased by 59.12%. This reduction underscores the effectiveness of the proposed measures in enhancing the efficiency of the system and minimizing energy losses. Additionally, the improvements in system reliability indices are significant, with SAIFI, SAIDI, and EENS showing notable enhancements.

The system reliability indices, including SAIFI, SAIDI, and EENS, have shown remarkable improvements, with enhancements of 91.2%, 95.54%, and 95.28%, respectively. These enhancements signify a substantial increase in the overall reliability and performance of the system. By achieving significant reductions in power losses and enhancing system reliability indices, the proposed measures demonstrate their efficacy in optimizing the operation of the power distribution system. These results highlight the importance of implementing strategic measures to enhance system efficiency and reliability, ultimately contributing to the seamless delivery of power to end-users.

4.4. DG Installation Cost

Both utilities and customers benefit from the integration of DGs into the existing system. In the case of the Guder town feeders, solar-based DG is preferable due to abundant natural resources, environmental advantages, and low maintenance and operating costs. The installation price of solar-based DG varies significantly over time. According to data obtained from [40], the average price of PV is projected to be 589 USD/KW for 2030 and 320 USD/KW for 2050. Therefore, considering these projected price changes, it is possible to estimate the current PV price based on this reference. Consequently, an average PV price for 2023 is estimated to be 683.15 USD/KW. Finally, with the consideration of case 3, the cost of DG installation is calculated and tabulated in Table 4.7.

Taking into account the various scenarios considered, particularly case 3, the cost of DG installation can be thoroughly assessed and tabulated for comprehensive analysis. This approach allows for a detailed examination of the financial implications associated with integrating DGs into the existing system, providing valuable insights into the feasibility and cost-effectiveness of such initiatives. Through careful consideration of installation costs and projected price trends, stakeholders can make informed decisions regarding the implementation of solar-based DG systems, ensuring both economic viability and environmental sustainability.

Table 4.7: Cost Summary of DGs

DGs size (MW)	Price per KW ($)	Total price ($)
DG1 = 1	683.15	683,150
DG2 = 1	683.15	683,150
DG3 = 1	683.15	683,150
DG4 = 1	683.15	683,150
DG5 = 1	683.15	683,150
Total		3,415,750

4.5. Cost of Energy Not Supplied Due to Power Loss and Interruptions

Installation of DG lowers lost costs and improves the performance of the distribution system.

Cost of Energy not supplied = Power not supplied * Electric tariff*Time (4.3)

Cost of Energy lost due to power loss = Power loss (Kw)*time (hr/year) *Electric tariff

= 611.9843 Kw*8760hr/yr*2birr/Kwh = 10,721,964.936 birr (average price of electricity is 2birr/kwh).

Cost of Energy not supplied due to interruption = EENS (Mwhr/yr) *year*tariff (birr/Kwh)

= 2368.307 MWh/yr*1yr*2birr/Kwh = 4,736,614 birr.

Total Cost of energy lost = Cost of energy lost due to interruption+ cost of energy lost due to power loss = (10,721,964.936 + 4,736,614) = 15,458,578.936 birr.

4.6. Cost of Energy Saved due to DG installation

Cost of energy saved due to power loss reduction = Power saved (Kw)*Time (hr/yr) *Electric tariff

= 309.2343Kw*8760hr/yr*2birr/Kwh = 5,417,784.936 birr.

Cost of energy saved due to interruption enhancement = Power saved (Mwhr/yr) *yr* Elec.tariff

= 2,256.549 Mwh/yr*1yr*2birr/Kwh = 4,513,098 birr.

Total Cost saved per year = cost of energy saved due to power loss + cost of energy saved due to interruption.

Total cost saved per year = (5,417,784.936 +4,513,098) = 9,930,882.936 birr.

CHAPTER FIVE

5. CONCLUSIONS, RECOMMENDATIONS AND FUTURE WORKS

5.1 CONCLUSIONS

In this study, renewable Distributed Generation (DG) is employed to enhance the reliability of the distribution system and mitigate power losses in the Guder distribution network. System modeling and simulation are conducted using ETAP and MATLAB software. The resulting system reliability indices, including SAIFI, SAIDI, and EENS, are obtained and analyzed. The recorded data reveals that the system experiences an average interruption frequency index (SAIFI) of 303.7458 f/customer/yr, an average interruption duration index (SAIDI) of 306.4240 hr/cust.yr, and total real and reactive power losses of 611.9843 KW and 323.8237 KVar, respectively. Furthermore, there is a significant amount of unsold energy amounting to 2,368.307 MWh/yr due to power outages, indicating substantial power unavailability and loss in the distribution network.

The existing system's reliability fails to meet the standards set by the Ethiopian Electric Agency, To address this issue and improve system reliability while reducing power losses, four DGs are integrated at optimal locations and sizes determined by the PSO algorithm. Upon integration, the system reliability indices of SAIFI, SAIDI, and EENS are notably decreased to 27.4968 f/customer/yr, 13.651 hr/cust.yr, and 111.7216 MWh/yr, respectively. This represents an improvement of 91.2%, 95.54%, and 95.28% for SAIFI, SAIDI, and EENS, respectively. Additionally, both real and reactive power losses are significantly reduced to 302.75 KW and 132.34 KVar, respectively, marking a decrease of 50.52% and 59.12%, respectively.

Furthermore, the study conducts cost estimation of DGs and evaluates the revenue obtained. Ultimately, the impact of DGs on the distribution network is comprehensively analyzed, and the results obtained before and after DG penetration are compared and assessed. Overall, the study successfully achieves its objectives and demonstrates the positive impact of DG integration on system reliability and power loss reduction.

5.2 RECOMMENDATIONS

Based on the findings of this study, the following are recommended for whom it may concern.

The electric utility company should encourage distributed generation technology not only for stand-alone power generation but also for grid-connected power generation, and even as a backup. Therefore, here it is recommended that the stakeholders should make encouragements to the government or concerned body to implement distributed generation in the distribution network.

Because DG integration has various negative impacts on distribution systems protection, updating the distribution systems protection must come before installing the DG. Therefore, it is strongly recommended here, as the implementation of automatic protection is necessary while integrating DG into the distribution network.

5.3 FUTURE WORKS

In order to further improve the reliability, and line loss reduction of the radial distribution system, simultaneous DG, and FACT device allocation is suggested here as future work.

In this study, only PV type DG was considered. It would be preferable to investigate alternative distributed generation for improving feeder reliability. And also further detail analysis of individual cost of PV components is recommended as future work.

REFERENCES

[1] A. Debrul, “By: Abeba Debru Teshome Advisor: Getachew Biru Worku (Dr.-Ing),” 2016.

[2] S. Manadhar, “Reliability Assessment Of Smart Distribution System And Analysis Of Automatic Line Switches,” 2013.

[3] A. Mehammed, “… Improvement By Intelligent Placement Of Distributed Generation (Dg) On Case Study Of Gonder City Power Distribution …,” 2020, [Online]. Available: Https://Ir.Bdu.Edu.Et/Handle/123456789/10785

[4] Bimrew Sendekie Belay, “Distribution System Reliability Assessment And Enhancement By Using Tie Switches And Sectionalizer’s,” הארץ, No. 8.5.2017, Pp. 2003–2005, 2022.

[5] B. K. Talukdar, “Electrical Distribution System (An Overview),” Int. J. Adv. Res. Innov. Ideas Educ., Vol. 5, No. 4, Pp. 22–33, 2019, [Online]. Available: Http://Ijariie.Com/Adminuploadpdf/Electrical_Distribution_System_An_Overview_Ijariie10571.Pdf

[6] 2017 Bewketu Getie, “Improvement Of Distribution System Reliability Using Distributed Generation And Circuit Reclosers (Case Study : Motta Substation),” 2020.

[7] C. L. T. Borges And D. M. Falcão, “Impact Of Distributed Generation Allocation And Sizing On Reliability, Losses And Voltage Profile,” 2003 Ieee Bol. Powertech - Conf. Proc., Vol. 2, Pp. 5–9, 2003, Doi: 10.1109/Ptc.2003.1304342.

[8] H. Mindaye, “Investigation And Reliability Improvement Of Radial Distribution System Using Flisr Technology / Case Study On Asella Distribution System /,” 2020.

[9] S. L. Braide, “Improved Reliability Analysis Of Electricity Power Supply To Port Harcourt Distribution Network,” Int. J. Eng. Sci. Invent., Vol. 7, No. 7, Pp. 23–36, 2018.

[10] A. M. Jaleel And M. K. Abd, “Reliability Evaluation Of Electric Distribution Network With Distributed Generation Integrated,” Int. J. Intell. Eng. Syst., Vol. 14, No. 5, Pp. 306–319, 2021, Doi: 10.22266/Ijies2021.1031.28.

[11] A. Hegvik, “Case Study Analysis Of Running Distributed Generators In Island Mode Effects On Reliability Of Supply,” No. June, 2012.

[12] C. Meteku, “Reliability Analysis Of 15kv Distribution System Network (Case Study: Addis Alem Substation Network),” No. January, 2020.

[13] 2015 Behailu Abebe, “Federal Democratic Republic Of Ethiopia Ministry Of Defense Defense University , College Of Engineering Office Of Postgraduate Programs And Research Minimization Of Harmonics Using Shunt Active Filter Minimization Of Harmonics Using Shunt Active Filter,” 2015.

[14] M. R. B. S., M. V. V K, And D. K. T. Veeramanju, “Evaluation Of Distributed Generation Impact On Reliability Of A Distribution System Using Digsilent Powerfactory,” Int. J. Innov. Technol. Explor. Eng., Vol. 9, No. 10, Pp. 381–389, 2020, Doi: 10.35940/Ijitee.J7586.0891020.

[15] A. Fernnandez Sarabia, “Impact Of Distributed Generation On Distribution System By,” Aalborg Univ. Denmark, No. June, P. 106, 2011.

[16] T. Adefarati And R. C. Bansal, “The Impacts Of Pv-Wind-Diesel-Electric Storage Hybrid System On The Reliability Of A Power System,” Energy Procedia, Vol. 105, Pp. 616–621, 2017, Doi: 10.1016/J.Egypro.2017.03.364.

[17] T. Adefarati And R. C. Bansal, “Integration Of Renewable Distributed Generators Into The Distribution System: A Review,” Iet Renew. Power Gener., Vol. 10, No. 7, Pp. 873–884, 2016, Doi: 10.1049/Iet-Rpg.2015.0378.

[18] A. Hailemariam, “Addis Ababa Institute Of Technology School Of Electrical And Computer Engineering Study On Planning Of Distribution System (A Case Study At Cotobie Substation) Electrical And Computer Engineering Study On Planning Of Distribution System (A Case Study A,” No. March, 2018.

[19] D. Maradin, L. Cerović, And T. Mjeda, “Economic Effects Of Renewable Energy Technologies,” Naše Gospod. Econ., Vol. 63, No. 2, Pp. 49–59, 2017, Doi: 10.1515/Ngoe-2017-0012.

[20] P. C. Maduforo, J. N. Emechebe, E. M. Eronu, And S. A. Benson, “Sensitivity Based Approach For The Optimal Sizing And Allocation Of Distributed Generation In A Radial

Network," Eur. J. Eng. Res. Sci., Vol. 5, No. 6, Pp. 751–756, 2020, Doi: 10.24018/Ejers.2020.5.6.1978.

[21] I. Hussain, F. Khan, I. Ahmad, S. Khan, And M. Saeed, "Power Loss Reduction Via Distributed Generation System Injected In A Radial Feeder," Mehran Univ. Res. J. Eng. Technol., Vol. 40, No. 1, Pp. 160–168, 2021, Doi: 10.22581/Muet1982.2101.15.

[22] S. Essallah, A. Bouallegue, And A. Khedher, "Optimal Sizing And Placement Of Dg Units In Radial Distribution System," Int. J. Renew. Energy Res., Vol. 8, No. 1, Pp. 166–177, 2018, Doi: 10.20508/Ijrer.V8i1.6666.G7291.

[23] M. H. Rind ++, M. K. Rathi, A. A. Hashmani, And A. A. Lashari ++, "Sindh Universityresearch Journal(Science Series) Optimal Placement And Sizing Of Dg In Radial Distribution System Using Pso Technique," Vol. 51, No. 04, Pp. 653–660, 2019, Doi: 10.26692/Sujo/2019.12.104.

[24] A. Hiluf, "Reliability Assessment Of Electrical Distribution Network U Sing Analytical Method : A C Ase S Tudy Of Maychew C Ity Distribution System," Vol. 9, No. 08, Pp. 977–985, 2020.

[25] A. A. Ogunsina, M. O. Petinrin, O. O. Petinrin, E. N. Offornedo, J. O. Petinrin, And G. O. Asaolu, "Optimal Distributed Generation Location And Sizing For Loss Minimization And Voltage Profile Optimization Using Ant Colony Algorithm," Sn Appl. Sci., Vol. 3, No. 2, 2021, Doi: 10.1007/S42452-021-04226-Y.

[26] K. Idowu, R. Uhunmwangho, E. C. N. Okafor, And A. Big-Alabo, "Reliability Improvement Study Of A Distribution Network With Distributed Generation," Appl. Model. Simul., Vol. 5, Pp. 53–65, 2021.

[27] T. K. . Okereafor, F. C.1, Idoniboyeobu, D.C.2, And Bala, "Open Access Analysis Of 33 / 11kv Rsu Injection Substation For Improved Performance With Distributed Generation (Dg) Units American Journal Of Engineering Research (Ajer)," No. 9, Pp. 301–316, 2017.

[28] G. Sasi Kumar, S. Sarat Kumar, And S. V. J. Kumar, "Dg Placement Using Loss

Sensitivity Factor Method For Loss Reduction And Reliability Improvement In Distribution System," Int. J. Eng. Technol., Vol. 7, No. 23, Pp. 236–240, 2018, [Online]. Available: Www.Sciencepubco.Com/Index.Php/Ijet

[29] D. L. Yadav And S. C. Choube, "Dg Placement In Distribution Systems Using Analytical Techniques," Int. J. Eng. Trends Technol., Vol. 69, No. 9, Pp. 236–241, 2021, Doi: 10.14445/22315381/Ijett-V69i9p228.

[30] Aditya Prasad Padhy, "Optimal Allocation And Size Selection Of Dispersed Generation In Radial Distribution System," Int. J. Eng. Res., Vol. V9, No. 07, Pp. 145–150, 2020, Doi: 10.17577/Ijertv9is070036.

[31] A. A. Arram, M. A. Farrag, And M. A. El-Sayed, "A Generalized Multistage Economic Planning Model For Distribution System Containing Dg Units," Int. J. Eng. Res. Dev., Vol. 11, No. 07, Pp. 2278–67, 2015.

[32] N. N. Gana And D. O. Akpootu, "Estimation Of Global Solar Radiation Using Four Sunshine Based Models In Kebbi, North-Western, Nigeria," Pelagia Res. Libr. Adv. Appl. Sci. Res., Vol. 4, No. 5, Pp. 409–421, 2013.

[33] F. S. Abu-Mouti And M. E. El-Hawary, "Optimal Distributed Generation Allocation And Sizing In Distribution Systems Via Artificial Bee Colony Algorithm," Ieee Trans. Power Deliv., Vol. 26, No. 4, Pp. 2090–2101, 2011, Doi: 10.1109/Tpwrd.2011.2158246.

[34] I. Techno, "Load Flow Analysis & Loss Allocation For Unbalanced Radial Power Distribution Systems," No. November, 2015.

[35] A. Meychw, "Hawassa University Insititute Of Technology School Of Electrical And Computer Engineering Second Year Post Graduate In Power System And Energy Engineering," 2021.

[36] M. U. Keerio, A. Ali, J. A. Laghari, And B. Shiana, "Minimization Of Power Loss In Radial Distribution Network Using Optimal Feeder Reconfiguration And Distributed Generation Allocation.," Pak. J. Sci., Vol. 71, No. 4, P. 179, 2019, [Online]. Available: Https://Scholar.Google.Com/Citations?View_Op=View_Citation&Hl=En&User=-

Oh82luaaaaj&Cstart=100&Pagesize=100&Citation_For_View=-Oh82luaaaaj:Dip1o2bni0gc

[37] "Design Of A Large Scale Solar Pv System," 2016.

[38] Ndagijimana And B. Kunjithapathan, "Design And Implementation Pv Energy System For Electrification Rural Areas," Int. J. Eng. Adv. Technol., Vol. 8, No. 5, Pp. 2340–2352, 2019.

[39] B. Asfaw, "Anomaly Detection Modeling In The School Of Graduate Studies Of Addis Ababa University In Partial Fulfillment Of The Requirements For The Degree Of Masters Of Science In Computer Science," 2007.

[40] T. Mekonnen, R. Bhandari, And V. Ramayya, "Modeling, Analysis And Optimization Of Grid-Integrated And Islanded Solar Pv Systems For The Ethiopian Residential Sector: Considering An Emerging Utility Tariff Plan For 2021 And Beyond," Energies, Vol. 14, No. 11, 2021, Doi: 10.3390/En14113360.

[41] S. Nikolova-Poceva, "Optimization Of Hybrid Renewable Energy System," J. Electr. Eng. Inf. Technol., Vol. 6, No. 1, Pp. 5–13, 2021, Doi: 10.51466/Jeeit2161181005np.

APPENDIX A: Reason of fault and interruption data for 2021/22

Month	**January, 2021**											
Feeder Name	**Reason of Interruptions**										Total Frequency	Total Duration
	DEF		DPSC		DTE		DTSC		OP			
	F	D	F	D	F	D	F	D	F	D	F	D
Ambo water	0	0	4	3.01	0	0	1	0.06	3	3.98	8.00	7.05
Ambo town	0	2	6	10.11	0	2	10	3.29	10	18.46	26.00	27.86
Guder town	0	0	5	6.21	0	0	6	0.64	3	3.28	14.00	10.13
Month	**February, 2021**											
Feeder Name	**Reason of Interruptions**										Total Frequency	Total Duration
	DEF		DPSC		DTE		DTSC		OP			
	F	D	F	D	F	D	F	D	F	D	F	D
Ambo water	1	2.57	4	3.32	0	0	6	0.49	10	19.54	21.00	25.92
Ambo town	3	3.45	11	15.38	6	2.57	7	2.6	6	2.14	33.00	34.14
Guder town	3	2.48	6	5.67	0	0	12	1.64	9	11.65	30.00	21.44
Month	**March 2021**											
Feeder Name	**Reason of Interruptions**										Total Frequency	Total Duration
	DEF		DPSC		DTE		DTSC		OP			
	F	D	F	D	F	D	F	D	F	D	F	D
Ambo water	0	0	1	0.58	1	0.06	0	0	4	4.26	6.00	4.90
Ambo town	2	2.61	7	11.93	1	2.05	10	2.89	11	2.51	31.00	29.99
Guder	0	0	12	10.11	2	0.22	8	0.84	7	3.11		

town											29.00	14.28
Month	**April 2021**											
Feeder Name	**Reason of Interruptions**										Total Frequency	Total Duration
	DEF		DPSC		DTE		DTSC		OP			
	F	D	F	D	F	D	F	D	F	D	F	D
Ambo water			4	4.27	2	0.14	4	2.68	5	4.73	15.00	11.82
Ambo town		3	8	6.8		4	7	2.41	11	7.37	26.00	23.58
Guder town	1	1.6	9	12.7	1	0.08	8	0.66	9	11.42	28.00	26.46
Month	**May 2021**											
Feeder Name	**Reason of Interruptions**										Total Frequency	Total Duration
	DEF		DPSC		DTE		DTSC		OP			
	F	D	F	D	F	D	F	D	F	D	F	D
Ambo water	1	14.98	8	9.82	1	0.06	1	0.37	5	10.8	16.00	36.03
Ambo town	2	7.77	10	14.61	1	2.08	10	3.7	2	2.48	25.00	30.64
Guder town	5	6.21	11	28.66	2	0.23	5	0.6	4	1.8	27.00	37.50
Month	**June 2021**											
Feeder Name	**Reason of Interruptions**										Total Frequency	Total Duration
	DEF		DPSC		DTE		DTSC		OP			
	F	D	F	D	F	D	F	D	F	D	F	D
Ambo water			6	22.76			4	8.48	1	0.08	11.00	31.32
Ambo town		2.05	8	8.05		4	1	2.05	6	3.85	15.00	20.00
Guder	3	2.13	27	20.74			6	0.6	2	2.69		

town											38.00	26.16
Month	**July 2021**											
Feeder Name	**Reason of Interruptions**										Total Frequency	Total Duration
	DEF		DPSC		DTE		DTSC		OP			
	F	D	F	D	F	D	F	D	F	D	F	D
Ambo water	0	0	2	0.78	0	0	4	2.61	4	5.88	10.00	9.27
Ambo town		0.49	9	4.51	0	0	4	1.92	12	7.84	25.00	14.76
Guder town	2	0.9	14	16.81	1	0.08	5	0.44	3	1.47	25.00	19.70
Month	**August 2021**											
Feeder Name	**Reason of Interruptions**										Total Frequency	Total Duration
	DEF		DPSC		DTE		DTSC		OP			
	F	D	F	D	F	D	F	D	F	D	F	D
Ambo water	0		2.0	2.15			2.0	0.16	4	4.97	8.00	7.28
Ambo town	2	2.00	3.00	3.81	2	2	12	4.30	10	11.83	29.00	23.94
Guder town	2	14.69	4.0	9.04	3	0.74	5.0	0.36	11	8.69	25.00	33.52
Month	**September 2021**											
Feeder Name	**Reason of Interruptions**										Total Frequency	Total Duration
	DEF		DPSC		DTE		DTSC		OP			
	F	D	F	D	F	D	F	D	F	D	F	D
Ambo water		2	6	15.3	3	2	8	2.16	9	3.1	36.00	32.91
Ambo town			4	13.3	1	0.35	6	0.16	7	1.1	18.00	14.91
Guder	3	13.0	6	19.58	2	0.76	12	2.03	7	4.7		

town		3									30.00	40.10
Month	**October 2021**											
Feeder Name	**Reason of Interruptions**										Total Frequency	Total Duration
	DEF		DPSC		DTE		DTSC		OP			
	F	D	F	D	F	D	F	D	F	D	F	D
Ambo water			1.0	1.76	1	0.78	4.0	0.87	4.0	15.21	10.00	18.62
Ambo town	2	2.00	4.00	4.79	2	2	12	4.04	12	11.00	32.00	31.83
Guder town			4.0	6.75	2	0.84	7	2.87	12	14.18	25.00	24.64
Month	**November 2021**											
Feeder Name	**Reason of Interruptions**										Total Frequency	Total Duration
	DEF		DPSC		DTE		DTSC		OP			
	F	D	F	D	F	D	F	D	F	D	F	D
Ambo water					1	0.85			1	0.53	2.00	1.38
Ambo town	2	2	3	3.08	2	2	10	4.87	5	4.52	19.00	16.47
Guder town			5	7.89	2	0.34	7	3.21	9	2.38	23.00	13.82
Month	**December 2021**											
Feeder Name	**Reason of Interruptions**										Total Frequency	Total Duration
	DEF		DPSC		DTE		DTSC		OP			
	F	D	F	D	F	D	F	D	F	D	F	D
Ambo water	0	0	3	7.01	0	0	1	0.06	2	0.41	6.00	7.48
Ambo town	0	2	12	15.9	0	2	11	3.05	11	8.12	34.00	31.07
Guder	1	0.28	6	3.13	1	0.08	3	0.24	5	10.68		

town											16.00	14.41
Month	**January 2022**											
Feeder Name	**Reason of Interruptions**										Total Frequency	Total Duration
	DEF		DPSC		DTE		DTSC		OP			
	F	D	F	D	F	D	F	D	F	D	F	D
Ambo water	1	0.7	1	1.88	1	0.07	3	0.17	9	11.41	15.00	14.23
Ambo town	2	3	8	6.53	2	3	10	3.72	7	8.35	29.00	24.60
Guder town	2	3.75	7	19.63	2	0.2	2	0.14	1	0.5	14.00	24.22
Month	**February 2022**											
Feeder Name	**Reason of Interruptions**										Total Frequency	Total Duration
	DEF		DPSC		DTE		DTSC		OP			
	F	D	F	D	F	D	F	D	F	D	F	D
Ambo water	3	14.45	2	4.02			1	0.12	5	6.41	11.00	25.00
Ambo town	2	3	12	17.08	2	3	6	3.37	8	12.04	30.00	38.49
Guder town	1	0.13	11	28.24					4	0.54	16.00	28.91
Month	**March 2022**											
Feeder Name	**Reason of Interruptions**										Total Frequency	Total Duration
	DEF		DPSC		DTE		DTSC		OP			
	F	D	F	D	F	D	F	D	F	D	F	D
Ambo water	2	5.33	4	4.85			1	0.08	14	33.59	21.00	43.85
Ambo town		3	6	5.25		3	2	3.18	9	21.38	17.00	35.81
Guder	5	3.73	17	21.16			1	0.07	6	1.76		

town											29.00	26.72
Month	**April 2022**											
Feeder Name	**Reason of Interruptions**										Total Frequency	Total Duration
	DEF		DPSC		DTE		DTSC		OP			
	F	D	F	D	F	D	F	D	F	D	F	D
Ambo water	1	3.95	5	6.76			2	0.06	14	24.31	22.00	35.08
Ambo town	3	3.87	13	20.43	2	3.11	4	3.17	13	18.99	35.00	49.57
Guder town	4	11.46	10	13.27	3	0.12	5	0.32	6	10.37	28.00	35.54
Month	**May 2022**											
Feeder Name	**Reason of Interruptions**										Total Frequency	Total Duration
	DEF		DPSC		DTE		DTSC		OP			
	F	D	F	D	F	D	F	D	F	D	F	D
Ambo water	4	2.31	2	5.95					6	15.68	12.00	23.94
Ambo town	9	26.33	13	20.57	6	3.63	1	3.2	16	8.93	45.00	62.66
Guder town	5	6.58	19	44.53	1	0.02	2	0.15	11	4.34	38.00	55.62
Month	**June 2022**											
Feeder Name	**Reason of Interruptions**										Total Frequency	Total Duration
	DEF		DPSC		DTE		DTSC		OP			
	F	D	F	D	F	D	F	D	F	D	F	D
Ambo water	3	1.89	2	2					10	4.85	15.00	8.74
Ambo town	10	10.11	13	12.83	2		4	0.2	19	7.3	48.00	30.44
Guder	12	14.5	16	10.59	1	0.12	4	0.41	17	15.83		

town		6									50.00	41.51
Month	**July 2022**											
Feeder Name	**Reason of Interruptions**										Total Frequency	Total Duration
	DEF		DPSC		DTE		DTSC		OP			
	F	D	F	D	F	D	F	D	F	D	F	D
Ambo water	2	2.75	2	2.12					3	5.99	7.00	10.86
Ambo town	5	3.16	8	7.18	7	3.73	3	3.44	14	5.42	37.00	22.93
Guder town	18	18.94	15	25.47	2	0.21	3	0.37	8	7.14	46.00	52.13
Month	**August 2022**											
Feeder Name	**Reason of Interruptions**										Total Frequency	Total Duration
	DEF		DPSC		DTE		DTSC		OP			
	F	D	F	D	F	D	F	D	F	D	F	D
Ambo water			2	6.53					6	13.72	8.00	20.25
Ambo town	1	0.46	3	5.39			4	1.18	9	3.46	17.00	10.49
Guder town	1	11	10	16.6			4	0.29	6	1.94	21.00	29.83
Month	**September 2022**											
Feeder Name	**Reason of Interruptions**										Total Frequency	Total Duration
	DEF		DPSC		DTE		DTSC		OP			
	F	D	F	D	F	D	F	D	F	D	F	D
Ambo water	0	0	1	2.16	1	0.06	0	0	2	0.68	4.00	2.90
Ambo town	2	3	15	18.94	4	3.18	10	3.9	10	10.55	41.00	39.57
Guder	3	8.41	21	11.4	3	0.32	1	0.08	7	3.75		

town											35.00	23.96
Month	**October 2022**											
Feeder Name	**Reason of Interruptions**										Total Frequency	Total Duration
	DEF		DPSC		DTE		DTSC		OP			
	F	D	F	D	F	D	F	D	F	D	F	D
Ambo water			2	10.92			2	0.15	3	0.71	7.00	11.78
Ambo town	3	8.1	8	5.26	2	3	14	3.97	5	3.91	32.00	24.24
Guder town	6	3.24	9	6.76	1	0.06	2	0.16	5	1.22	23.00	11.44
Month	**November 2022**											
Feeder Name	**Reason of Interruptions**										Total Frequency	Total Duration
	DEF		DPSC		DTE		DTSC		OP			
	F	D	F	D	F	D	F	D	F	D	F	D
Ambo water			2	1.42			5	3.72	5	12.97	12.00	18.11
Ambo town	2	3	10	15.72	2	3	9	6.54	9	5.72	32.00	33.98
Guder town	5	3.63	20	10.59	1	0.28	5	0.3	5	8.41	36.00	23.21
Month	**December 2022**											
Feeder Name	**Reason of Interruptions**										Total Frequency	Total Duration
	DEF		DPSC		DTE		DTSC		OP			
	F	D	F	D	F	D	F	D	F	D	F	D
Ambo water	1	1.03	3	2.5	2	0.12	3	0.35	9	5.99	18.00	9.99
Ambo town	2	3	8	8.66	4	3.2	7	3.3	3	3.03	24.00	21.19
Guder	2	9.73	7	12.88	3	0.2	5	0.34	2	1.04		

town											19.00	24.19

APPENDIX B: Basic characteristics of Suniva ART245-60-3-1PV [41]

The Suniva ART245-60-3-1 PV module data	**Values**	**Unit**
Maximum power(P_{max})	240	W
Maximum power point voltage(V_{mpp})	30.65	V
Maximum power point current(I_{mpp})	7.82	A
Open circuit voltage(V_{oc})	37.08	V
Short circuit current(I_{Sc})	8.33	A
Voltage temperature coefficient(β)	-0.332	%/C
Current temperature coefficient(α)	0.036	%/C
Efficiency	14.9	%
Module Temperature	-40 to +90	°C
Irradiance	1000	W/m^2
Length	165.3	Cm
Width	98.2	Cm
Area	1.62	Cm^2
Max system DC voltage	1000	V
Warranty	25	Years

APPENDIX C: Technical specifications of the chosen inverter[41]

Inverter model:- PVS800-57-1000KW-C	
DC Inputs	
Maximum input power (P_{PVmax})	1000KW
DC voltage range ($V_{mpp\ DC}$)	600 to 850V
Maximum DC voltage ($V_{max\ DC}$)	1100V
Maximum DC current ($I_{max\ DC}$)	1710A
Number of protected DC inputs	8 to 20(+/-)
AC Output	
Nominal power($P_{nom\ AC}$)	1000 KW
Maximum output power	1200 KW
Power at 0.9 pf	950 KW
Nominal AC current($I_{nom\ AC}$)	1445 A
Nominal output voltage($V_{nom\ AC}$)	400 V
Frequency	50/60 HZ
Maximum efficiency	98.8%
External auxiliary voltage	230 V, 50 HZ

APPENDIX D: Calculated line and load data of the selected feeder

Sending end	Receiving end	Resistance (r)	Reactance (x)	Conductor type	Length (Km)	Pload (Mw)	Qload (Mvar)
1	2	0.801	0.2015	AAC-95(mm^2)	2.7	0	0
1	3	0.0463	0.0487	AAC-95(mm^2)	0.15	0.3378	0.25335
2	4	0.2	0.21	AAC-95(mm^2)	0.65	0.111	0.08325
4	5	0.0154	0.00162	AAC-95(mm^2)	0.05	0	0
5	6	0.031	0.0324	AAC-95(mm^2)	0.1	0	0
5	7	0.01543	0.1622	AAC-95(mm^2)	0.5	0	0
7	8	0.1543	0.1622	AAC-95(mm^2)	0.5	0	0
8	9	0.1543	0.1622	AAC-95(mm^2)	0.5	0.305	0.22875
8	10	0.0926	0.0973	AAC-95(mm^2)	0.3	0	0
10	11	0.031	0.0324	AAC-95(mm^2)	0.1	0	0
11	12	0.0926	0.0973	AAC-95(mm^2)	0.3	0.016	0.012
12	13	0.1079	0.1135	AAC-95(mm^2)	0.35	0	0
13	14	0.0463	0.0487	AAC-95(mm^2)	0.15	0	0
14	15	0.031	0.0324	AAC-95(mm^2)	0.1	0.027	0.02025
14	16	0.031	0.0324	AAC-95(mm^2)	0.1	0	0
16	17	0.0154	0.0162	AAC-95(mm^2)	0.05	0.020	0.015
16	18	0.0154	0.0162	AAC-95(mm^2)	0.05	0	0
18	19	0.031	0.0324	AAC-95(mm^2)	0.1	0	0
18	20	0.0771	0.0811	AAC-95(mm^2)	0.25	0	0
20	21	0.0154	0.0162	AAC-95(mm^2)	0.05	0	0
20	22	0.1079	0.1135	AAC-95(mm^2)	0.35	0	0
7	23	0.0154	0.0162	AAC-95(mm^2)	0.05	0.0795	0.0596
23	24	0.0463	0.0487	AAC-95(mm^2)	0.15	0	0
23	25	0.0154	0.0162	AAC-95(mm^2)	0.05	0.029	0.02175

25	26	0.0154	0.0162	AAC-95(mm^2)	0.05	0.025	0.01875
26	27	0.0463	0.0487	AAC-95(mm^2)	0.15	0	0
26	28	0.216	0.2271	AAC-95(mm^2)	0.7	0.0732	0.0549
28	29	0.1736	0.1041	AAC-50(mm^2)	0.3	0	0
28	30	0.26	0.156	AAC-50(mm^2)	0.45	0.060	0.045
30	31	0.116	0.069	AAC-50(mm^2)	0.2	0.014	0.0105
30	32	0.05785	0.0347	AAC-50(mm^2)	0.1	0.0250	0.1875
32	33	0.1446	0.0868	AAC-50(mm^2)	0.25	0.1425	0.1068
33	34	0.0289	0.0174	AAC-50(mm^2)	0.05	0.017	0.01275
34	35	0.0289	0.0174	AAC-50(mm^2)	0.05	0.3126	0.23445
35	36	0.0289	0.0174	AAC-50(mm^2)	0.05	0.1047	0.0785
35	37	0.1446	0.0868	AAC-50(mm^2)	0.25	0.010	0.0075
37	38	0.116	0.069	AAC-50(mm^2)	0.2	0.093	0.06975
37	39	0.0868	0.0521	AAC-50(mm^2)	0.15	0.0984	0.0938
36	40	0.0868	0.0521	AAC-50(mm^2)	0.15	0.092	0.069
40	41	0.05785	0.0347	AAC-50(mm^2)	0.1	0.009	0.00675
40	42	0.0289	0.0174	AAC-50(mm^2)	0.05	0.0155	0.011625
42	43	0.1736	0.1041	AAC-50(mm^2)	0.3	0	0
43	44	0.1446	0.0868	AAC-50(mm^2)	0.25	0.049	0.03675
44	45	0.116	0.069	AAC-50(mm^2)	0.2	0.061	0.04575
44	46	0.2025	0.1215	AAC-50(mm^2)	0.35	0.053	0.03975
46	47	0.1736	0.1041	AAC-50(mm^2)	0.3	0.041	0.03075
46	48	0.05785	0.0347	AAC-50(mm^2)	0.1	0.045	0.03375
47	49	0.0868	0.0521	AAC-50(mm^2)	0.15	0	0
46	50	0.2314	0.1388	AAC-50(mm^2)	0.4	0.013	0.0975
33	51	0.116	0.069	AAC-50(mm^2)	0.2	0	0
51	52	0.05785	0.0347	AAC-50(mm^2)	0.1	0.012	0.009

51	53	0.1736	0.1041	AAC-50(mm^2)	0.3	0	0
53	54	0.05785	0.0347	AAC-50(mm^2)	0.1	0.009	0.00625
54	55	0.116	0.069	AAC-50(mm^2)	0.2	0	0
54	56	0.05785	0.0347	AAC-50(mm^2)	0.1	0.045	0.03375
56	57	0.0868	0.0521	AAC-50(mm^2)	0.15	0.033	0.02475
57	58	0.2025	0.1215	AAC-50(mm^2)	0.35	0	0
25	59	0.2025	0.1215	AAC-50(mm^2)	0.35	0.1236	0.0927
59	60	0.2314	0.1388	AAC-50(mm^2)	0.4	0	0
60	61	0.1446	0.0868	AAC-50(mm^2)	0.25	0.363	0.27225
60	62	0.0289	0.0174	AAC-50(mm^2)	0.05	0	0
62	63	0.2314	0.1388	AAC-50(mm^2)	0.4	0.1173	0.0879
62	64	0.116	0.069	AAC-50(mm^2)	0.2	0.069	0.05175
64	65	0.0289	0.0174	AAC-50(mm^2)	0.05	0	0
65	66	0.0289	0.0174	AAC-50(mm^2)	0.05	0	0
65	67	0.0289	0.0174	AAC-50(mm^2)	0.05	0.017	0.01275
67	68	0.0868	0.0521	AAC-50(mm^2)	0.15	0.013	0.00975
68	69	0.116	0.069	AAC-50(mm^2)	0.2	0	0
68	70	0.116	0.069	AAC-50(mm^2)	0.2	0.035	0.02625
70	71	0.1446	0.0868	AAC-50(mm^2)	0.25	0.1862	0.13965
70	72	0.2893	0.1735	AAC-50(mm^2)	0.5	0.2618	0.19635
67	73	0.116	0.069	AAC-50(mm^2)	0.2	0.2444	0.1683
73	74	0.1446	0.0868	AAC-50(mm^2)	0.25	0.031	0.02325
74	75	0.3182	0.191	AAC-50(mm^2)	0.55	0.1299	0.0974
74	76	0.0289	0.0174	AAC-50(mm^2)	0.05	0	0
76	77	0.0868	0.0521	AAC-50(mm^2)	0.15	0	0
77	78	0.0868	0.0521	AAC-50(mm^2)	0.15	0.077	0.05775
77	79	0.0289	0.0174	AAC-50(mm^2)	0.05	0.015	0.01125

79	80	0.05785	0.0347	AAC-50(mm^2)	0.1	0	0
80	81	0.0868	0.0521	AAC-50(mm^2)	0.15	0.021	0.01575
80	82	0.0868	0.0521	AAC-50(mm^2)	0.15	0	0
79	83	0.0289	0.0174	AAC-50(mm^2)	0.05	0.1533	0.1149
83	84	0.116	0.069	AAC-50(mm^2)	0.2	0	0
83	85	0.0289	0.0174	AAC-50(mm^2)	0.05	0.287	0.21525
85	86	0.05785	0.0347	AAC-50(mm^2)	0.1	0	0
86	87	0.1446	0.0868	AAC-50(mm^2)	0.25	0.2866	0.21495
87	88	0.05785	0.0347	AAC-50(mm^2)	0.1	0	0
85	89	0.0289	0.0174	AAC-50(mm^2)	0.05	0.011	0.00825
89	90	0.0289	0.0174	AAC-50(mm^2)	0.05	0.4874	0.36555
90	91	0.05785	0.0347	AAC-50(mm^2)	0.1	0	0
91	92	0.0289	0.0174	AAC-50(mm^2)	0.05	0.155	0.1163
92	93	0.1446	0.0868	AAC-50(mm^2)	0.25	0	0
93	94	0.1736	0.1041	AAC-50(mm^2)	0.3	0.241	0.18075
94	95	0.1446	0.0868	AAC-50(mm^2)	0.25	0.085	0.06375
94	96	0.0868	0.0521	AAC-50(mm^2)	0.15	0.015	0.01125
96	97	0.05785	0.0347	AAC-50(mm^2)	0.1	0	0
97	98	0.0868	0.0521	AAC-50(mm^2)	0.15	0.023	0.01725
98	99	0.2025	0.1215	AAC-50(mm^2)	0.35	0.041	0.03075
93	100	0.1446	0.0868	AAC-50(mm^2)	0.25	0	0
100	101	0.0868	0.0521	AAC-50(mm^2)	0.15	0.2622	0.1966
101	102	0.2025	0.1215	AAC-50(mm^2)	0.35	0	0
91	103	0.2893	0.1735	AAC-50(mm^2)	0.5	0.157	0.11775
103	104	0.116	0.069	AAC-50(mm^2)	0.2	0.181	0.13575
104	105	0.2314	0.1388	AAC-50(mm^2)	0.4	0	0
104	106	0.1446	0.0868	AAC-50(mm^2)	0.25	0.169	0.12675

106	107	0.05785	0.0347	AAC-50(mm^2)	0.1	0.111	0.08325
107	108	0.1446	0.0868	AAC-50(mm^2)	0.25	0.0669	0.050
107	109	0.05785	0.0347	AAC-50(mm^2)	0.1	0	0
89	110	0.2603	0.1562	AAC-50(mm^2)	0.45	0	0
110	111	0.2314	0.1388	AAC-50(mm^2)	0.4	0.033	0.02475
111	112	0.0289	0.0174	AAC-50(mm^2)	0.05	0.101	0.07575
111	113	0.0289	0.0174	AAC-50(mm^2)	0.05	0.011	0.00825
110	114	0.116	0.069	AAC-50(mm^2)	0.2	0.1677	0.1277
114	115	0.2025	0.1215	AAC-50(mm^2)	0.35	0.1362	0.10215
115	116	0.0289	0.0174	AAC-50(mm^2)	0.05	0.018	0.0135
116	117	0.0868	0.0521	AAC-50(mm^2)	0.15	0.041	0.03075
116	118	0.0289	0.0174	AAC-50(mm^2)	0.05	0.039	0.02925